Embryonic Development of the Axial Column in the Little Skate, *Leucoraja erinacea*

Katharine E. Criswell,[1,2]* Michael I. Coates,[1] and J. Andrew Gillis[2,3]

[1]*Department of Organismal Biology and Anatomy, University of Chicago, Chicago, Illinois*
[2]*Marine Biological Laboratory, Woods Hole, Massachusetts*
[3]*Department of Zoology, University of Cambridge, Cambridge, UK*

ABSTRACT The morphological patterns and molecular mechanisms of vertebral column development are well understood in bony fishes (osteichthyans). However, vertebral column morphology in elasmobranch chondrichthyans (e.g., sharks and skates) differs from that of osteichthyans, and its development has not been extensively studied. Here, we characterize vertebral development in an elasmobranch fish, the little skate, *Leucoraja erinacea*, using microCT, paraffin histology, and whole-mount skeletal preparations. Vertebral development begins with the condensation of mesenchyme, first around the notochord, and subsequently around the neural tube and caudal artery and vein. Mesenchyme surrounding the notochord differentiates into a continuous sheath of spindle-shaped cells, which forms the precursor to the mineralized areolar calcification of the centrum. Mesenchyme around the neural tube and caudal artery/vein becomes united by a population of mesenchymal cells that condenses lateral to the sheath of spindle-shaped cells, with this mesenchymal complex eventually differentiating into the hyaline cartilage of the future neural arches, hemal arches, and outer centrum. The initially continuous layers of areolar tissue and outer hyaline cartilage eventually subdivide into discrete centra and arches, with the notochord constricted in the center of each vertebra by a late-forming "inner layer" of hyaline cartilage, and by a ring of areolar calcification located medial to the outer vertebral cartilage. The vertebrae of elasmobranchs are distinct among vertebrates, both in terms of their composition (i.e., with centra consisting of up to three tissues layers—an inner cartilage layer, a calcified areolar ring, and an outer layer of hyaline cartilage), and their mode of development (i.e., the subdivision of arch and outer centrum cartilage from an initially continuous layer of hyaline cartilage). Given the evident variation in patterns of vertebral construction, broad taxon sampling, and comparative developmental analyses are required to understand the diversity of mechanisms at work in the developing axial skeleton of vertebrates. J. Morphol. 278:300–320, 2017. © 2017 Wiley Periodicals, Inc.

KEY WORDS: elasmobranch; vertebral column; development; microCT; skate

RESEARCH HIGHLIGHTS

- Skate vertebrae form via a continuous condensation of mesenchyme that differentiates into cartilage and later subdivides.
- Vertebral centra consist of three layers: an inner cartilage, a middle areolar calcification, and an outer hyaline cartilage.

INTRODUCTION

The vertebral column is a key component of the vertebrate skeleton, providing structural support for the skull and appendicular skeleton, as well as protection for the spinal cord and axial blood vessels. A vertebral column can include a notochord and/or series of centra, neural, and hemal arches and spines, zygapophyses to articulate one vertebra to another, and transverse processes, perhaps articulating with ribs (Fig. 1). Vertebrae are a defining feature of the vertebrate clade, but different components of the vertebral skeleton, namely the arches and centra, have evolved independently of one another, are variable in their construction, and might therefore be patterned by separate developmental mechanisms (Arratia et al., 2001). To gain insight into the developmental and evolutionary basis of axial column morphological variation, broad taxon sampling of developmental and anatomical

Contract grant sponsors: Henry Hinds Fund for Graduate Student Research in Evolutionary Biology, a Company of Biologists Travelling Fellowship, a Marine Biological Laboratory/University of Chicago Graduate Research Award, and a National Science Foundation Doctoral Dissertation Improvement (to K. E. C.); Contract grant number: DEB-1501749; Contract grant sponsor: National Science Foundation (to M. I. C.); Contract grant number: DEB-0917922; Contract grant sponsor: Royal Society University Research Fellowship (J. A. G.); Contract grant number: UF130182; Contract grant sponsors: Plum Foundation John E. Dowling and Laura and Arthur Colwin Endowed Summer Research Fellowships at the Marine Biological Laboratory, and by a grant from the University of Cambridge Isaac Newton Trust [14.23z].

*Correspondence to: Katharine E. Criswell, Department of Organismal Biology and Anatomy, University of Chicago, Chicago, IL. E-mail:kcriswell@uchicago.edu

Received 3 August 2016; Revised 11 November 2016; Accepted 29 November 2016.

Published online 31 January 2017 in Wiley Online Library (wileyonlinelibrary.com). DOI 10.1002/jmor.20637

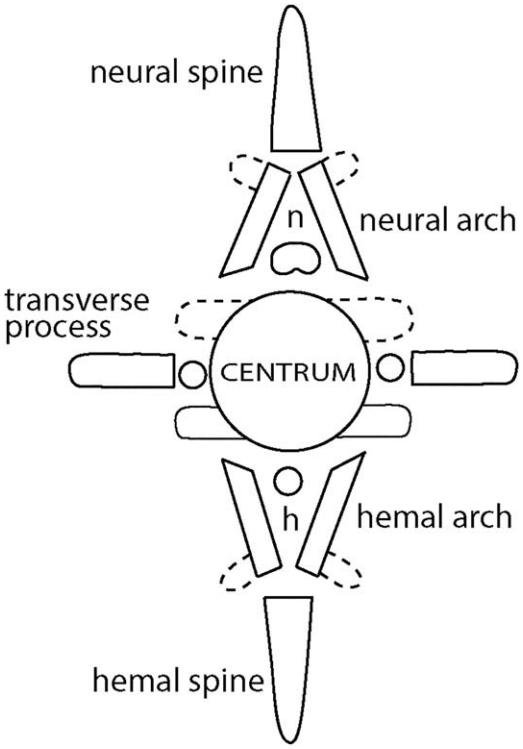

Fig. 1. The ideal, typical vertebra redrawn from Owen (1848), showing the neural and hemal arches and spines, transverse processes, and centrum. n, neural canal; h, hemal canal.

data within vertebrates, and particularly, within jawed vertebrates (gnathostomes), is needed. However, at present, most data on vertebral column development have been collected from a handful of osteichthyan taxa (i.e., bony fishes and tetrapods) (Fleming et al., 2015). There is a notable paucity of developmental data for the vertebral columns of chondrichthyans (cartilaginous fishes—sharks, skates, rays, and holocephalans), and this results in a biased and incomplete picture of vertebral column evolution within gnathostomes and vertebrates as a whole.

The onset of vertebral development begins in a similar fashion in all taxa studied to date, when a subpopulation of mesodermal cells undergoes an epithelial to mesenchymal transformation from the ventral somites, and migrates medially as sclerotome (Gadow and Abbott, 1895; Christ and Wilting, 1992). These sclerotomal cells are thought to condense at dorsolateral and ventrolateral positions relative to the notochord, and form the basidorsal (neural arch) and basiventral (hemal arch) rudiments. After sclerotome migration and condensation, vertebral development, and centrum formation in particular, is more varied. Depending on the taxon, centra may arise via a combination of four general processes: 1) Through arch primordia encircling the notochord (arcocentra); 2) through sclerotomal cells that invade and chondrify within the notochord sheath (chordacentra); 3) through chondrocytes that differentiate around the notochord sheath (holocentra); or 4) through direct ossification outside the notochord sheath (autocentra) (Arratia et al., 2001).

The developmental mechanisms and tissues underlying vertebral formation differ greatly between different vertebrate clades. In teleost fishes (actinopterygians) the vertebrae are composed of acellular bone, in which bone-forming osteoblasts are not incorporated into the skeletal tissue after bone matrix is secreted (Hall, 2005). Centra in zebrafish (*Danio rerio*) form before the arches, by nine days post fertilization, and vertebrae ossify directly without cartilaginous precursors (Fleming et al., 2004; Bensimon-Brito et al., 2012). The arches form from sclerotomal cells that condense both dorsal to and ventral to the notochord, but the centra form from bone matrix that seems to be deposited by the notochord itself (Fleming et al., 2004). In Atlantic salmon (*Salmo salar*), neural and hemal arch cartilages form first and are then encased in bone, with centra developing later through four layers of mineralization. These four layers include the chordacentrum, which mineralizes within the notochord sheath, a thin, continuous perinotochordal layer that covers the notochord, an outer layer of laminin bone making up each centrum, and lastly, cancellous bone with longitudinal trabeculae (Nordvik et al., 2005; Wang et al., 2013). As a third example, chordacentra in the Japanese medaka (*Oryzias latipes*) develop within the notochord sheath prior to being surrounded by perichordal bone (Ekanayake and Hall, 1987).

In tetrapods (salamander, chick, and mouse), vertebrae have been documented to form entirely from migrating sclerotomal cells that condense around the notochord to form a perichordal tube of tissue that then differentiates into individual vertebral units (Bagnall et al., 1988; Christ and Wilting, 1992; Piekarski and Olsson, 2014). In chick (*Gallus gallus*), the ventral portion of the somite has been fate mapped to specific vertebral components, with the medial-most cell population contributing to the centra, the dorsal sclerotomal cells giving rise to neural spines, and the lateral portion of the sclerotome making up the remainder of the neural arches and ribs (Bagnall et al., 1988; Christ et al., 2000). In the axolotl (*Ambystoma mexicanum*), a urodele amphibian, fate mapping of somites three to five shows somitic contributions to all vertebral parts, including the centra, arches, and intervertebral discs (Piekarski and Olsson, 2014). This variation in vertebral development across vertebrates highlights the need for more data from the sister group of osteichthyans, the cartilaginous fishes (chondrichthyans).

Extant chondrichthyans belong to one of two lineages: the holocephalans and the elasmobranchs. Extant holocephalans comprise the chimaeroids, a small group of largely deep-sea fishes, while extant elasmobranchs include skates and rays (collectively

known as batoids) and sharks. Vertebral column anatomy in adult elasmobranchs differs markedly from that of osteichthyans. The elasmobranch vertebral column consists of a zipper-like series of neural and intercalary arches dorsally, along with centrum cartilages that support transverse processes precaudally and hemal arches caudally (see Fig. 1; Daniel, 1922). A series of mediolaterally flattened neural spines sits in between vertebral boundaries on the dorsal-most surface of the vertebral column throughout the length of the body. The arches consist of a core of hyaline cartilage covered by a mosaic of blocks of calcified tissue called tesserae in adults (Dean and Summers, 2006). Most elasmobranchs have mineralized chordacentra (centra formed within the notochord sheath), in which cells differentiate into dense rings within the fibrous notochord sheath and are surrounded by apatite in their intercellular spaces, forming a highly cellular, netlike mineralized tissue called areolar calcification (Gadow and Abbott, 1895; Applegate, 1967; Dean and Summers, 2006). These centra take on an hourglass shape, expanding anteriorly and posteriorly, and constrict the notochord considerably at their center, with remnants of the notochord persisting at the intervertebral boundaries. Caudal diplospondyly, a condition in which two vertebrae correspond to each myomere and set of spinal nerves, is well known in many sharks (Ridewood, 1899), but occurs in batoids as well.

Within elasmobranchs, vertebral morphology is variable. In the broadnose seven-gill shark (*Notorynchus cepedianus*), the notochord is surrounded by an unsegmented cartilaginous tube and supports thin, mineralized ring centra that persist into adulthood (Daniel, 1922). In the porbeagle shark (*Lamna nasus*), the hammerhead (*Sphyrna blochii*), the basking shark (*Cetorhinus maximus*), and the guitarfish (*Rhinobatos productus*), heavily mineralized centra form within the fibrous notochord sheath and expand throughout ontogeny to engulf the neural and hemal arches (Ridewood, 1921; Daniel, 1922; Goodrich, 1930). In many elasmobranchs, such as the horn shark (*Heterodontus francisci*), small-spotted catshark (*Scyliorhinus canicula*), little skate (*Leucoraja erinacea)*, and some rays (e.g., *Myliobatis aquila*), the cartilage of the arches expands dorsally and ventrally to envelop the calcified centra (Hasse, 1879; Daniel, 1922).

Current understanding of elasmobranch vertebral development derives largely from historical studies on sharks, with only sparse data from skates and rays (for shark data see Gegenbaur, 1872; Hasse, 1879; Klaatsch, 1893a,b, 1895; Gadow and Abbott, 1895; Goodrich, 1958; and see Klaatsch, 1893b for a discussion of vertebral development in the electric ray *Torpedo ocellata*). These studies demonstrated that the initiation of shark vertebral development proceeds, as in osteichthyans, with the migration of sclerotomal cells toward the notochord sheath. The notochord sheath thickens into a ring of fibrous, spindle-shaped cells, surrounded by a thin membrane, the elastica externa. Sclerotomal mesenchyme is thought to both condense around the notochord, forming cartilaginous units that give rise to the neural and hemal arches, and migrate through the perforated elastica externa and into the fibrous sheath where it differentiates into the cartilage of the centrum.

Historically, sharks have been used as representatives of generalized, and by implication ancestral, gnathostome anatomical conditions (e.g., Goodrich, 1930). As a result, the classic, and most used, model of vertebral construction, based on vertebral development in sharks, was widely applied to gnathostomes as a whole (Gadow and Abbott, 1895; Gadow, 1933). It suggests that for all gnathostomes each vertebral unit is composed of four pairs of embryonic cartilages, or "arcualia": two pairs of dorsal elements (basidorsals and interdorsals) and two pairs of ventral elements (basiventrals and interventrals; Gadow and Abbott, 1895). The basidorsals form the adult neural arches and, when present, the dorsal intercalary arches, and the basiventrals form the hemal arches and ventral intercalary arches. Several key works have pointed out that the "Arcualia Theory" is not compatible with published evidence for osteichthyan (Schaeffer, 1967) and acanthodian fishes (Miles, 1970) and the theory has been rejected outright for tetrapods (Williams, 1959). Despite this apparent incongruity, the simplistic arcualia model, and its associated terminology, remains influential and is often used to describe the vertebrae of non-tetrapod gnathostomes in the paleontological and comparative anatomical literature (Jarvik, 1980a,b; Arratia et al., 2001). Additionally, it is unclear whether all elasmobranchs develop according to Gadow and Abbott's (1895) model or whether some clades, such as batoids, deviate from this pattern.

It is clear from the bias of developmental studies towards osteichthyans (zebrafish, chick, and mouse), the lack of studies on vertebral column development in cartilaginous fishes utilizing modern microtomographic (microCT) techniques, and the confusion over current embryological terminology and models, that tests of historical hypotheses and a renewed focus on vertebral column evolution are needed. To reconstruct sequences of character evolution for the gnathostome vertebral column, that is, to determine which developmental processes are general for gnathostomes, and to distinguish between homologous and homoplastic vertebral structures, it is necessary to collect morphological and developmental data from numerous osteichthyan and chondrichthyan taxa. Additionally, an assessment of whether the processes of vertebral development that have been described in sharks are representative for all elasmobranchs requires data on axial column development in batoids. Here, we use computed tomography,

histology, and whole mount skeletal preparation to visualize the embryonic development of the axial column in a batoid elasmobranch, the little skate *Leucoraja erinacea*. Crucially, the use of high-resolution microCT scans allows for interpretations of detailed anatomy in three dimensions that have not previously been possible. The little skate is an emerging model for studies of gnathostome development and evolution, and as such, the methods employed here will be broadly useful to researchers studying other anatomical systems.

MATERIALS AND METHODS

Animal Collection, Husbandry, and Fixation

Developmental series of the little skate, *Leucoraja erinacea* (Mitchill, 1825), from Stages 27 to 34, were obtained from the Marine Resources Center (MRC) at the Marine Biological Laboratory in Woods Hole, MA. Embryonic stages correspond to those described in the staging table of the winter skate, *Leucoraja ocellata* (Maxwell et al., 2008). Little skate embryos reach Stage 27 after approximately four weeks of development at 18°C and have developed small pectoral and pelvic fins. By Stage 34, after approximately 5 months of development, embryos are close to hatching, with dark pigmentation and little external yolk remaining. Embryos were maintained at approximately 18°C in seawater while at the MRC, until Stage 27, and were then maintained at 15°C in reconstituted Instant Ocean (Aquarium Systems) on at 12-h light-dark cycle. On reaching the appropriate developmental stage, embryos were removed from their keratinous egg cases using a razor blade and euthanized with an overdose of MS-2222 (Ethyl 3-aminobenzoate methanesulfonate—Sigma-Aldrich) (1 g/l bath). Embryos were then fixed for 24–48 h in 4% paraformaldehyde, rinsed three times in 1X phosphate buffered saline (3 × 5 min), and graded into either 100% methanol (MeOH) or ethanol (EtOH) through an ascending series (25%, 50%, 75%, and 100% in 1X PBS, 5min/rinse) and stored at −20°C.

MicroCT Scanning

Embryos of all stages were stained with Iodine Potassium Iodide (IKI) (2% w/v iodine and 1% w/v potassium iodide in water), diluted to 10% in water, for three to five days to provide contrast to soft tissues. Two Stage 31 embryos were stained with 5% w/v phosphomolybdic acid (PMA) in MeOH for five days. Both IKI and PMA provide contrast to soft tissues, but PMA is actually taken up by cartilage, and presents as an even, mid-range gray tone in the CT slices.

Embryos at Stages 28–30 and 32–33 were microCT scanned at the University of Texas at Austin CT Laboratory (UTCT) using an XRadia microXCT 400 scanner. Embryos at Stages 30–34 were microCT scanned in the Department of Organismal Biology at the University of Chicago, using a General Electric Phoenix v|tome|x 240 MicroCT scanner with two X-ray tubes and 16′ × 16′ detector panel of 2,048 × 2,048 pixel resolution (see Table 1 for scanning parameters). The 180 kV 15W high-power NanoFocus tube achieves a maximum voxel resolution of 0.5 μm and can scan organisms in a size range of 15 cm in length by 12 cm in diameter. Resulting scans were segmented using Mimics versions 17.0 and 18.0 (Materialise, Leuven, Belgium).

Skeletal Preparations

A second series of embryos, corresponding to the stages discussed above, were cleared and stained with Alcian blue to visualize the proteoglycan-rich matrix present in vertebral cartilage. This protocol was based on a standard clearing and staining protocol for fishes (Klymkowsky and Hanken, 1991) that was optimized for use on elasmobranch fishes (Gillis et al., 2009). Alcian blue-stained embryos were imaged using a Leica MZFLIII microscope with a Nikon D5000 camera, and the Camera Control Pro software. White balance was adjusted in Adobe Photoshop CS6 using the levels tool; no other editing was performed.

TABLE 1. MicroCT scanning parameters for skate embryos scanned and used in this study

Stage	# Scanned	Stain	kV	μA	Timing	Voxel size
28	2	IKI	60	167	3 s	2.90
			70	143	2 s	3.08
29	1	IKI	60	167	3 s	2.47
30	4	IKI	100	100	2 s	2.63
			70	143	3 s	2.93
			70	143	3 s	2.93
			60	167	2.5	3.08
31	3	PMA	100	100	2 s	2.95
		PMA	40	250	4 s	2.79
		IKI	110	70	2 s	3.12
32	1 PC	IKI	100	100	2 s	2.58
	2 C		60	167	2 s	4.16
			60	167	2 s	4.16
33	2 C	IKI	60	167	1.5 sec	4.99
34	1 PC	IKI	80	70	4 sec	3.76
	1 C		100	100	2 sec	3.08

One scan sampling each separate morphological state was figured here. Images from additional scans were not included because they did not differ significantly in their morphology from other scans of similarly staged embryos. C = caudal region, IKI = iodine potassium iodide, kV = kilovolts, PC = precaudal region, PMA = phosphomolybdic acid, μA = microamps, voxel size in micrometers.

Paraffin Histology and Staining

A third series of embryos (two specimens per stage) was paraffin embedded and sectioned for histochemical staining with Hematoxylin, Eosin, and Alcian blue (HEA). Hematoxylin is a positively charged, basic dye that stains acidic structures, such as cell nuclei containing DNA and RNA, with a dark violet to bluish color (Fischer et al., 2008). Eosin is a negatively charged, acidic dye that stains basic tissues that include proteins, such as cytoplasm and sometimes extracellular matrix, pink. As mentioned previously, Alcian blue was used to identify proteoglycan-rich extracellular matrix in section. Older embryos with heavily calcified vertebrae and dermal denticles (Stage 32 and above) were demineralized in 10% ethylenediaminetetraacetic acid (EDTA) for 14 days prior to embedding. The embedding process consisted of three 20-min rinses in histosol (National Diagnostics), followed by two 30-min rinses in a 50:50 paraffin:histosol solution at 67°C. The tissue was then placed in 100% paraffin overnight at 67°C, and during the following day the paraffin was changed five times before the tissue was placed in embedding blocks and positioned. The tissue was sectioned in transverse or sagittal orientation at a thickness of 8 μm using a Microm HM 330 microtome with Thermo Fisher HP 35 coated blades.

HEA-staining was performed on sections according to established protocols (Gillis et al., 2009). Sections were imaged with a Zeiss Axioplan microscope, Nikon D5000 camera, and Camera Control Pro software. White balance was adjusted in Adobe Photoshop CS6 using the levels tool; no other editing was performed.

RESULTS

Here, we describe the embryonic morphology of the little skate vertebral column through a series of embryos, beginning with the earliest appearance of recognizable vertebral tissue, and ending with

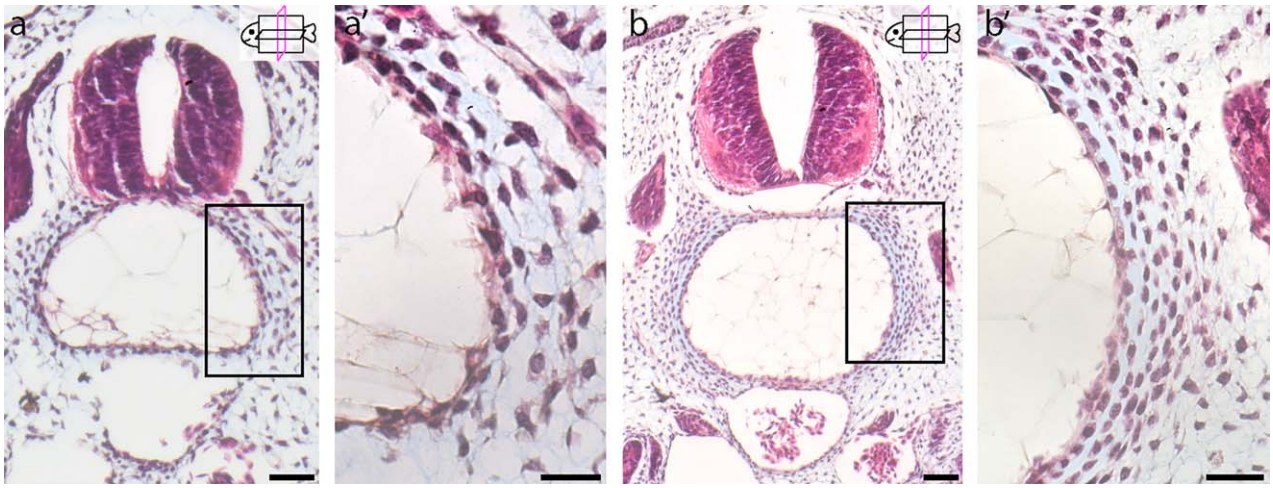

Fig. 2. *Leucoraja erinacea*, embryonic vertebral morphology in Stage 27 embryos. **a**) cross section through an early HEA-stained Stage 27 embryo; **a′**) 20× magnification of cells surrounding the notochord in a; **b**) cross section through a late HEA-stained Stage 27 embryo; **b′**) 20× magnification of mesenchymal cells condensing around the notochord in b. Icons in upper right corner indicate plane of section. Scale bars represent 50 μm for a and b, and 25 μm for a′ and b′.

the fully differentiated vertebral skeleton. Following this sequential description, we provide a summary of the patterns observed in skate and a schematic that tracks the different layers of vertebral tissue through development.

Stage 27

At the start of Stage 27, loose mesenchyme appears to surround the notochord as a single layer of cells just peripheral to the notochord epithelium (Fig. 2a,a′). As development progresses additional mesenchymal cells condense around the notochord, up to five cells thick, to form a continuous layer that extends the length of the body (Fig. 2b,b′).

Stages 28–29

Incipient vertebral structures (neural and hemal arch mesenchyme) appear at Stage 28 and remain largely unchanged through Stage 29. The notochord sheath consists of an inner layer that is approximately two cells thick, surrounded by an outer layer of elongate, spindle-shaped cells arranged concentrically around the notochord and forming a thickened fibrous tube (Fig. 3a–c′). The spindle-shaped cells surrounding the notochord are embedded in Alcian blue-stained (and therefore presumably proteoglycan-rich) extracellular matrix, and microCT scans show that both neural and hemal arch mesenchyme and this layer of spindle-shaped cells are deposited as unsegmented tubes along the entire anterior–posterior axis (Fig. 3d–f). Mesenchymal cells condense dorsal and ventral to the notochord, to form the nascent neural and hemal arches, but at this point the mesenchyme has not yet reached the dorsal-most portion of the neural tube (Fig. 3g–k). Sagittal and horizontal sections reveal that the notochord is unconstricted (Fig. 3f,l).

Precaudally, small lateral condensations of mesenchyme, also continuous along the anterior–posterior axis of the notochord, begin to form transverse processes (Fig. 3c,c′). The dorsal aorta is present as a wide canal just ventral to the notochord. Dorsal root ganglia are large and teardrop-shaped, spaced close to one another, and have corresponding nerves extending posteroventrally down the length of the incipient vertebrae (Fig. 3d,e). Nervous tissue stains brightly with IKI in young embryos (Fig. 3b,h,l), providing clear markers of each axial segment, even when the vertebral tissue is continuous.

Caudally, development is largely contemporaneous with the precaudal region. Mesenchymal cells extend ventrally and condense around the caudal artery and vein, but these cells are not spindle-shaped in appearance and the matrix surrounding these cells does not stain with Alcian blue. The dorsal-most and ventral-most extensions of condensed mesenchyme are thicker than the rest of the tissue, giving it a bulging square shape in cross section (Fig. 3g,h,i). The incipient neural arch tissue extends dorsally from the base, near the notochord, but does not yet fully enclose the neural tube, as in the precaudal region. The dorsal root ganglia and spinal nerves are spaced farther apart caudally than in the precaudal region (Fig. 3k), foreshadowing that each set of nerves will correspond with two vertebrae in the caudal region, as opposed to a single vertebral unit in the precaudal region. The caudal artery and vein are large, with small foramina forming in the hemal arch cartilage to admit blood vessels (Fig. 3j,k). In Stages 28 and 29 wholemount cleared and stained specimens, Alcian blue-stained cartilage is not yet visible (not shown).

Stage 30

In the precaudal region in Stage 30 skate embryos, the neural tube, dorsal root ganglia, and

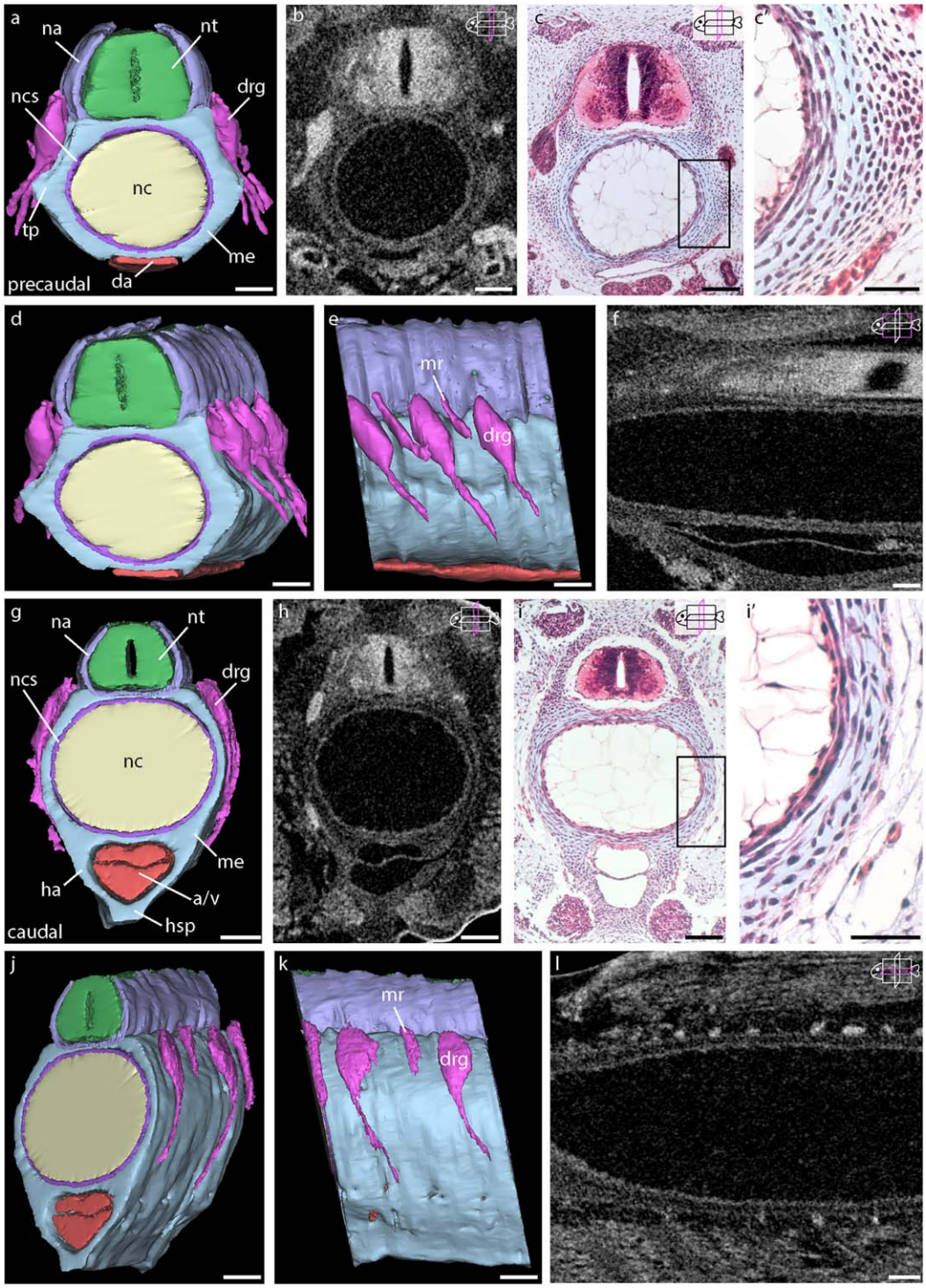

Fig. 3. *Leucoraja erinacea*, embryonic vertebral morphology in Stages 28–29 embryos. **a**) anterior view of a CT reconstruction of the precaudal vertebrae; **b**) transverse section through the IKI-stained CT scan; **c**) transverse section stained with HEA, showing the thickened layer of spindle-shaped cells; **c′**) 20× magnification of the layer of spindle-shaped cells; **d**) anterolateral view of the precaudal CT reconstruction; **e**) lateral view of the precaudal CT reconstruction; **f**) sagittal section through the precaudal CT scan; **g**) anterior view of the caudal CT reconstruction; **h**) transverse section of the caudal CT scan; **i**) transverse section through the caudal vertebrae stained with HEA; **i′**) 20× magnification of the layer of spindle-shaped cells; **j**) anterolateral view of the caudal CT reconstruction; **k**) lateral view of the caudal CT reconstruction; **l**) sagittal section of the caudal CT scan. a/v, caudal artery and vein, da, dorsal aorta, drg, dorsal root ganglion, ha, hemal arch, hsp, hemal spine, me, mesenchymal sheath, mr, motor nerve root, na, neural arch, nc, notochord, ncs, notochord sheath, nt, neural tube, tp, transverse process. Icons in upper right corner indicate plane of section. Scale bars represent 100 μm for most images; scale bars represent 50 μm for c′ and i′.

spinal nerves remain unchanged from previous stages (Fig. 4a–e). Vertebral tissues at Stage 30 are very similar to those at Stage 29, though several subtle differences are observed. The sheath of spindle-shaped cells remains continuous, but has increased in thickness (Fig. 4f). Hints of future notochord constriction (and, eventually, vertebral boundaries) can be seen in sagittal and horizontal sections in both the precaudal and caudal regions as the notochord begins to segmentally decrease in size (Fig. 4f–g). The morphology of the caudal vertebrae is similar to that of the precaudal region, with a thickened layer of spindle-shaped cells (Fig. 4h–k), but with spinal nerves that are more widely separated, indicating future diplospondyly, in which each myotomal segment will eventually include two vertebrae instead of one (Fig. 4k–l).

Mesenchymal condensations surrounding the neural tube dorsally and caudal artery and vein ventrally now meet at the dorsal and ventral midline, respectively, to fully enclose the axial column (Fig. 4c,m–n). At this stage, the tissue of the transverse processes has condensed, but remains undifferentiated (Fig. 4b,c,c′). Compared to Stage 29, the tissue connecting the nascent hemal arches to the hemal spines has thinned slightly (Fig. 4h,k–l).

Stage 31

During Stage 31, the condensed mesenchyme of the neural and hemal arches differentiates into cartilage and is continuous with the cartilage enveloping the notochord and its surrounding layer of spindle-shaped cells. The notochord continues to decrease in diameter relative to the vertebrae, and boundaries between vertebral elements (centrum cartilages, neural, and intercalary arches) become apparent. Late in Stage 31, the cartilage surrounding the notochord becomes restricted to each vertebral segment, and thins at presumptive vertebral boundaries. This cartilaginous tube remains continuous, but variations in thickness can be seen on the outer surface of the centrum cartilage in CT reconstructions (Figs. 5g,i and 6d,e).

Precaudally, the mesenchyme of the neural arches and spines has differentiated into cartilage and stains strongly with Alcian blue (Fig. 5a–d). Boundaries are now present separating the arches and cartilage of the centra, and clear spinal nerve foramina have developed (Fig. 5c,e–f). The neural arch tissue still appears continuous throughout the anterior–posterior axis in microCT scans, but arches have begun to form shallow grooves, corresponding with myotomal segments (Fig. 5g–i). In sagittal section, boundaries separating the neural and intercalary arches are visible (Fig. 5j). The transverse processes are well formed by late Stage 31, extending posterolaterally, and have begun to segment by subdividing medially, although the lateral-most extensions remain continuous (Fig. 5b,c,f,i).

In the thicker cartilaginous regions (centra), a middle layer of eosin-stained tissue can be seen in section, which represents the first appearance of the mineralized areolar tissue (Fig. 5c,c′). In the thinner, intervertebral regions, the layer of spindle-shaped cells has increased in thickness, forming dense, concentric rings around the notochord (Fig. 5f,f′). In one CT-scan of a PMA-stained embryo, small bands of tissue seem to intrude into the notochord, forming on the inside of the notochord sheath, and at the widest part of the notochord in each myotomal segment (Fig. 5b,d,h). These rings are only present precaudally and are positioned just medial to and in line with the grooves visible on the surface of the outer cartilage, suggesting that they may have a role in directing the subdivision of the continuous cartilage. However, these structures have not yet been observed in any other specimens, indicating either that this specimen might be anomalous, or that this tissue is ephemeral, being present only for a short time in development.

Embryonic morphology of the caudal vertebrae differs slightly from the precaudal vertebrae by the end of Stage 31. The neural and intercalary arches have begun to separate, with small slits forming in the cartilage, although they remain continuous at the level of the neural spines and at their bases (Fig. 6a–e). The centrum cartilages have also begun to thicken at intervals corresponding to each myotomal boundary, but the grooves representing incipient vertebral boundaries are not as deep as in the precaudal region (Fig. 6e). Both the fibrous intervertebral regions and the widest parts of the centrum are similar to the precaudal vertebrae, with a ring representing the early areolar tissue medially and Alcian blue-stained cartilage in the outer layer (Fig. 6f,g,g′,h,h′). Segmental constriction of the notochord has increased from Stage 30, with clear decreases in notochord diameter in each myotomal segment (Fig. 6i,j). Hemal spines remain as a continuous mesenchymal condensation that appears discontinuous with the hemal arches (Fig. 6e–h). Dorsal root ganglia and spinal nerves remain broadly spaced, in contrast to their close precaudal positioning (Fig. 6d,e).

Stages 32–33

All components of the vertebral column are present by Stage 32, and neural arches, intercalary arches, and centra have all completely segmented (Figs. 7 and 8). The arch cartilages now consist of clearly defined neural arches, which are long and thin in the precaudal region, and more substantial intercalary arches that contain spinal nerve foramina (Fig. 7a–d,g). The neural spines have also begun to segment, but remain connected at their bases (Fig. 7d,e). The transverse processes on the centrum cartilages are clearly pronounced, and extend both anteriorly at a slight ventral angle, and posterodorsally. The posterior portion of

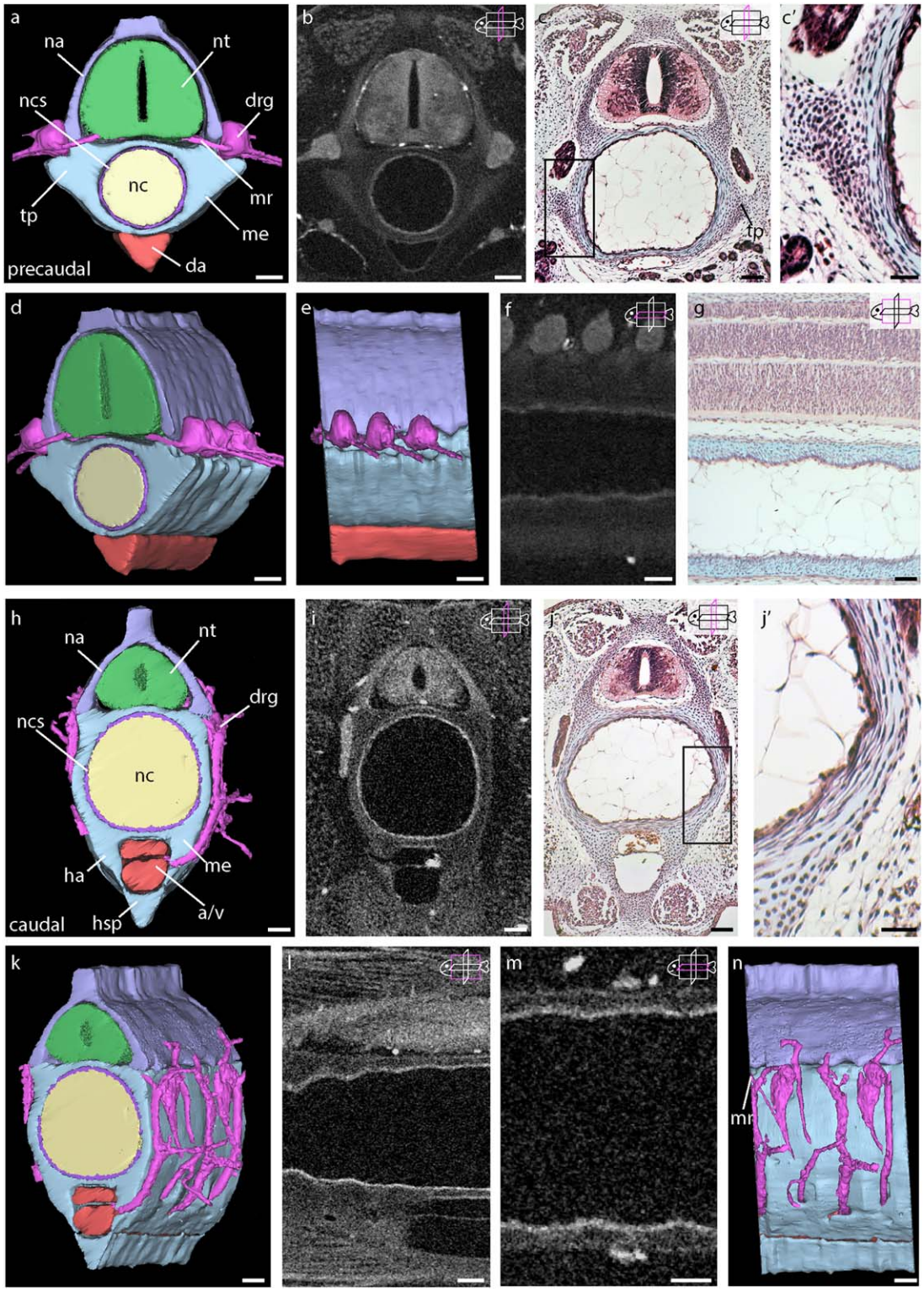

Fig. 4. *Leucoraja erinacea*, embryonic vertebral morphology in Stage 30 embryos. **a**) anterior view of a CT reconstruction of the precaudal vertebrae; **b**) transverse section through the IKI-stained CT scan; **c**) transverse section stained with HEA showing the layer of spindle-shaped cells and condensed mesenchyme of the transverse processes; **c′**) 20× zoom of the layer of spindle-shaped cells; **d**) anterolateral view of a CT reconstruction of the precaudal vertebrae; **e**) lateral view of a CT reconstruction of the precaudal vertebrae; **f**) horizontal section through a CT scan of the precaudal vertebrae; **g**) sagittal section stained with HEA; **h**) anterior view of a CT reconstruction of the caudal vertebrae; **i**) transverse section through a CT scan of the caudal vertebrae; **j**) transverse section through the caudal vertebrae, stained with HEA; **j′**) 20× zoom of the layer of spindle-shaped cells shown in j; **k**) anterolateral view of a CT reconstruction of caudal vertebrae; **l**) sagittal section through a CT scan of the caudal vertebrae; **m**) horizontal section of a CT scan through the caudal vertebrae; **n**) lateral view of a CT reconstruction of caudal vertebrae. a/v, caudal artery and vein, da, dorsal aorta, drg, dorsal root ganglion, ha, hemal arch, hsp, hemal spine, me, mesenchymal sheath, mr, motor nerve root, na, neural arch, nc, notochord, ncs, notochord sheath, nt, neural tube, tp, transverse process. Icons in upper right corner indicate plane of section. Scale bars are 100 μm for most images, and 50 μm for c′ and j′.

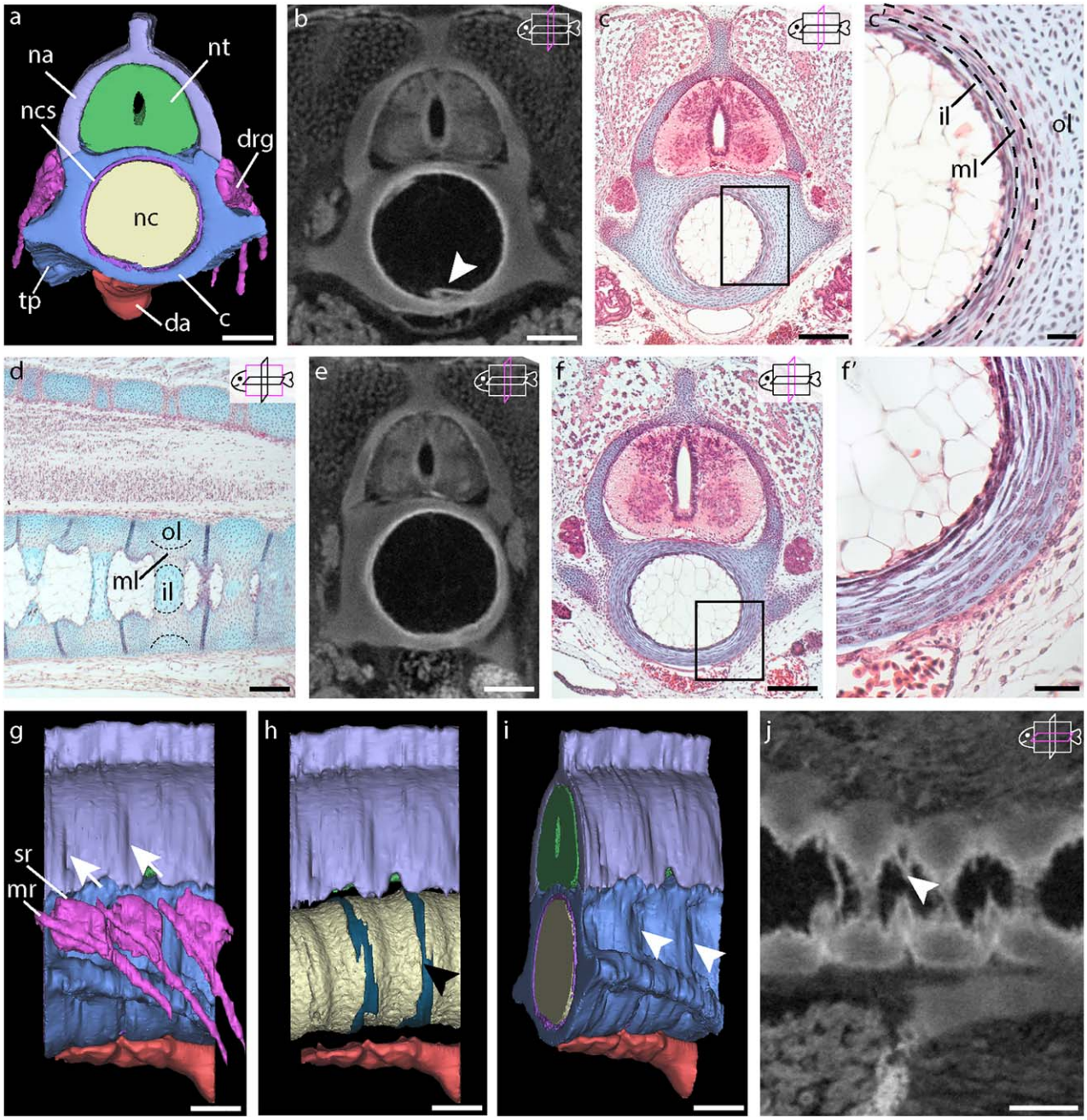

Fig. 5. *Leucoraja erinacea*, precaudal embryonic vertebral morphology in Stage 31 embryos. **a**) anterior view of a CT reconstruction of the precaudal vertebrae; **b**) transverse section through the PMA-stained CT scan showing the widest part of the vertebra, arrowhead refers to notochord band; **c**) transverse section stained with HEA, showing the thickened continuous cartilage; **c′**) 20× zoom of the centrum cartilage, dashed lines indicate first appearance of areolar tissue; **d**) sagittal section through a late Stage 31 skate embryo stained with HEA, dashed lines indicate areolar tissue; **e**) transverse section through the CT scan showing the morphology of the intervertebral region; **f**) transverse section stained with HEA, showing the narrow, fibrous nature of the intervertebral region; **f′**) 20× zoom of the fibrous rings; **g**) lateral view of the CT reconstruction showing dorsal root ganglia and spinal nerves, arrows indicate grooves of incipient arch boundaries; **h**) lateral view of the CT reconstruction with centrum cartilage removed, arrowhead indicates notochord band; **i**) anterolateral view of the CT reconstruction showing the grooves of incipient vertebral boundaries, arrowheads depict location of grooves indicating incipient subdivision; **j**) horizontal section through the CT scan, arrowhead indicates notochord band. da, dorsal aorta, drg, dorsal root ganglion, c, cartilage, il, inner layer of cartilage, ml, middle layer of centrum/areolar calcification, mr, motor nerve root, na, neural arch, ncs, notochord sheath, nt, neural tube, ol, outer layer of hyaline cartilage, sr, sensory nerve root, tp, transverse process. Icons in upper right corner indicate plane of section. Scale bars are 200 μm for most images, scale bars are 100 μm for c′ and f′.

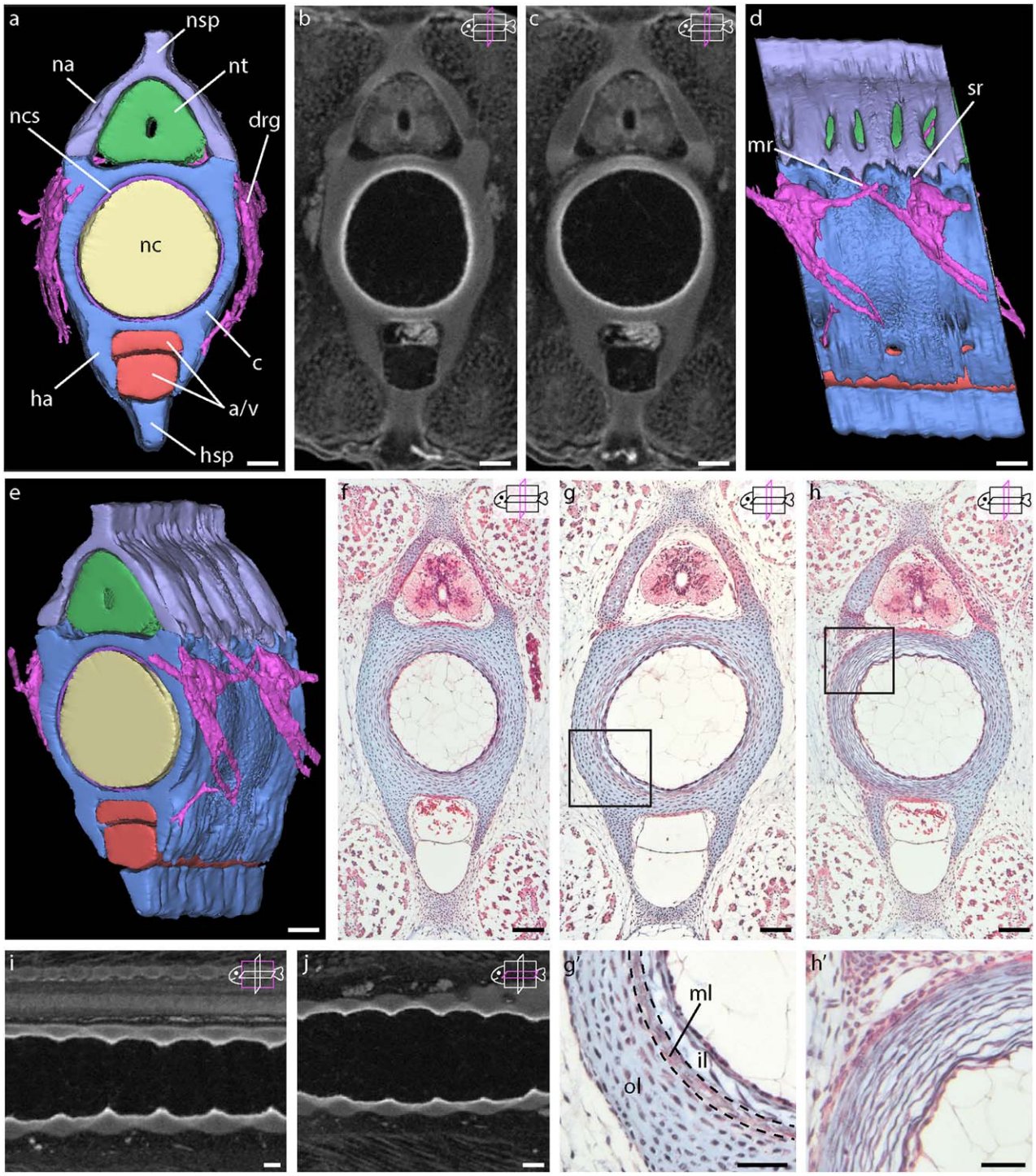

Fig. 6. *Leucoraja erinacea*, caudal embryonic vertebral morphology in Stage 31 embryos. **a**) anterior view of a CT reconstruction of the caudal vertebrae; **b**) transverse section through the PMA-stained CT scan showing the widest part of the vertebrae; **c**) transverse section through a CT scan showing the narrowest portion, where the continuous cartilage will eventually subdivide; **d**) lateral view of the CT reconstruction; **e**) anterolateral view of the CT reconstruction; **f**) transverse section stained with HEA, showing the thickened continuous cartilage; **g**) transverse section showing the early formation of the middle layer of tissue that will eventually form the areolar calcification; **g′**) 20× magnification showing the incipient centrum; **h**) transverse oblique section showing the fibrous nature of the intervertebral tissue; **h′**) 20× magnification of the fibrous intervertebral ring; **i**) sagittal section through the CT scan showing segmental constriction of the notochord; and **j**) horizontal section through the CT scan showing segmental thickening and constriction of the vertebral cartilage surrounding the notochord. a/v, caudal artery and vein, c, cartilage, drg, dorsal root ganglion, ha, hemal arch, hsp, hemal spine, il, inner layer of cartilage, ml, middle layer of centrum/areolar calcification, mr, motor nerve root, na, neural arch, nc, notochord, ncs, notochord sheath, nsp, neural spine, nt, neural tube, ol, outer layer of hyaline cartilage, sr, spinal nerve root. Scale bars represent 100 μm for most images; scale bars represent 50 μm for g′ and h′.

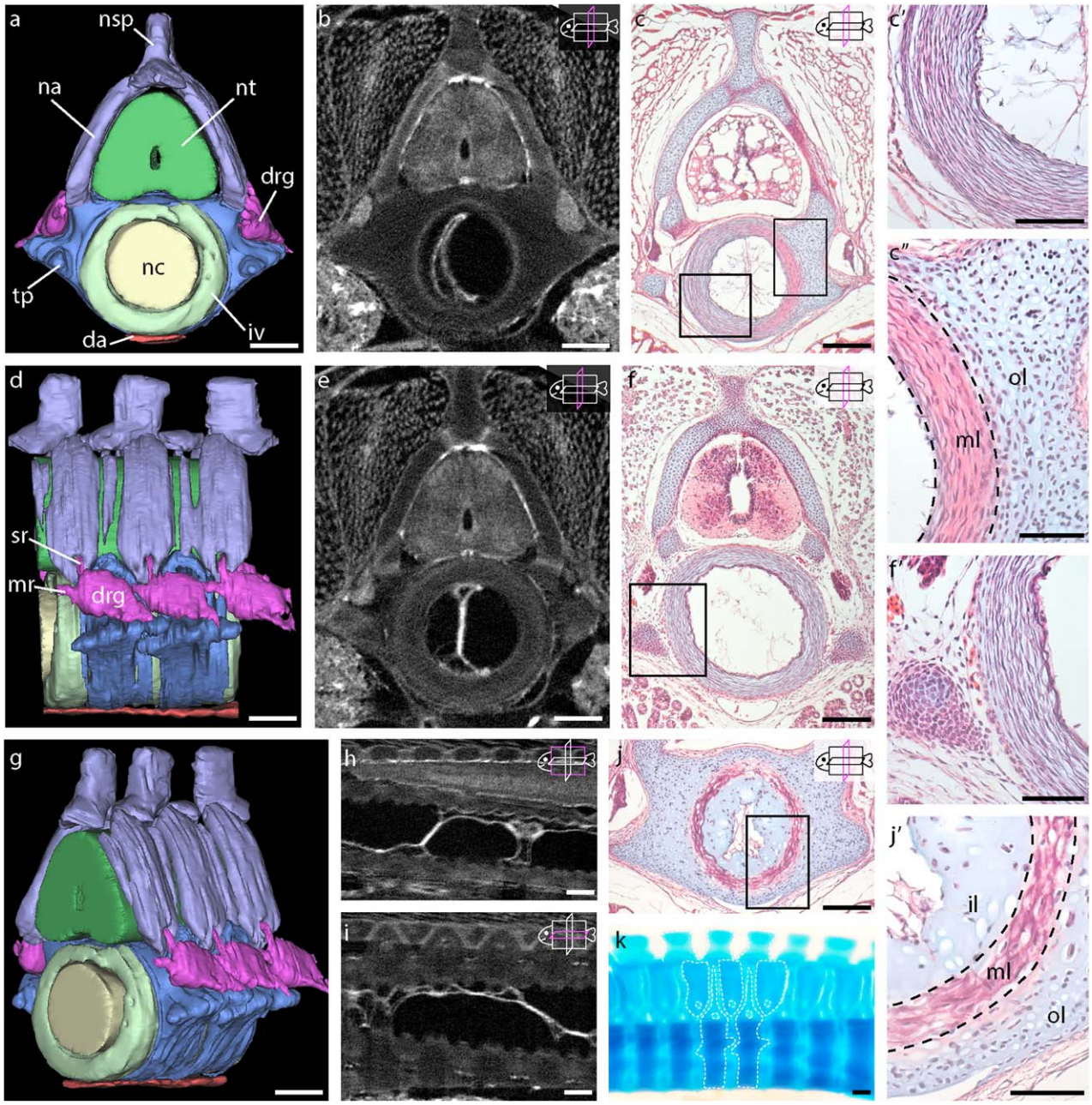

Fig. 7. *Leucoraja erinacea*, precaudal embryonic vertebral morphology in Stage 32 embryos. **a**) anterior view of a CT reconstruction of the precaudal vertebrae; **b**) transverse section through the IKI-stained CT scan showing the widest part of the vertebrae; **c**) transverse oblique section stained with HEA; **c′**) 20× magnification of the fibrous ring shown in c; **c″**) 20× magnification of the mineralizing centrum and outer layer of cartilage shown in c, dashed lines indicate middle layer/areolar calcification; **d**) lateral view of the CT scan of the precaudal vertebrae; **e**) transverse section through the intervertebral region of the CT scan; **f**) transverse section through the intervertebral region stained with HEA; **f′**) 20× magnification of the fibrous ring and transverse process shown in f; **g**) anterolateral view of the CT reconstruction; **h**) sagittal section of the CT scan; **i**) horizontal section of the CT scan; **j**) transverse section through a slightly older embryo showing the early areolar calcification of the centrum; **j′**) 20× magnification of the developing centrum, dashed lines indicate middle layer/areolar calcification; **k**) skeletal preparation of precaudal vertebrae in lateral view showing well developed transverse processes. da, dorsal aorta, drg, dorsal root ganglion, il, inner layer of cartilage, iv, intervertebral region, ml, middle layer of centrum/areolar calcification, mr, motor nerve root, na, neural arch, nsp, neural spine, nt, neural tube, ol, outer layer of hyaline cartilage, sr, spinal nerve root, tp, transverse process. Icons in upper right corner indicate plane of section. Scale bars represent 200 μm for most images; scale bars represent 100 μm for c′, c″, f′, and j′.

the transverse process overlaps the anterior portion of the subsequent transverse process (Fig. 7d–g).

The developing areolar tissue, stained with eosin in section, is clearly visible in CT scans, in HEA-stained sections, and in whole mount skeletal preparations. In

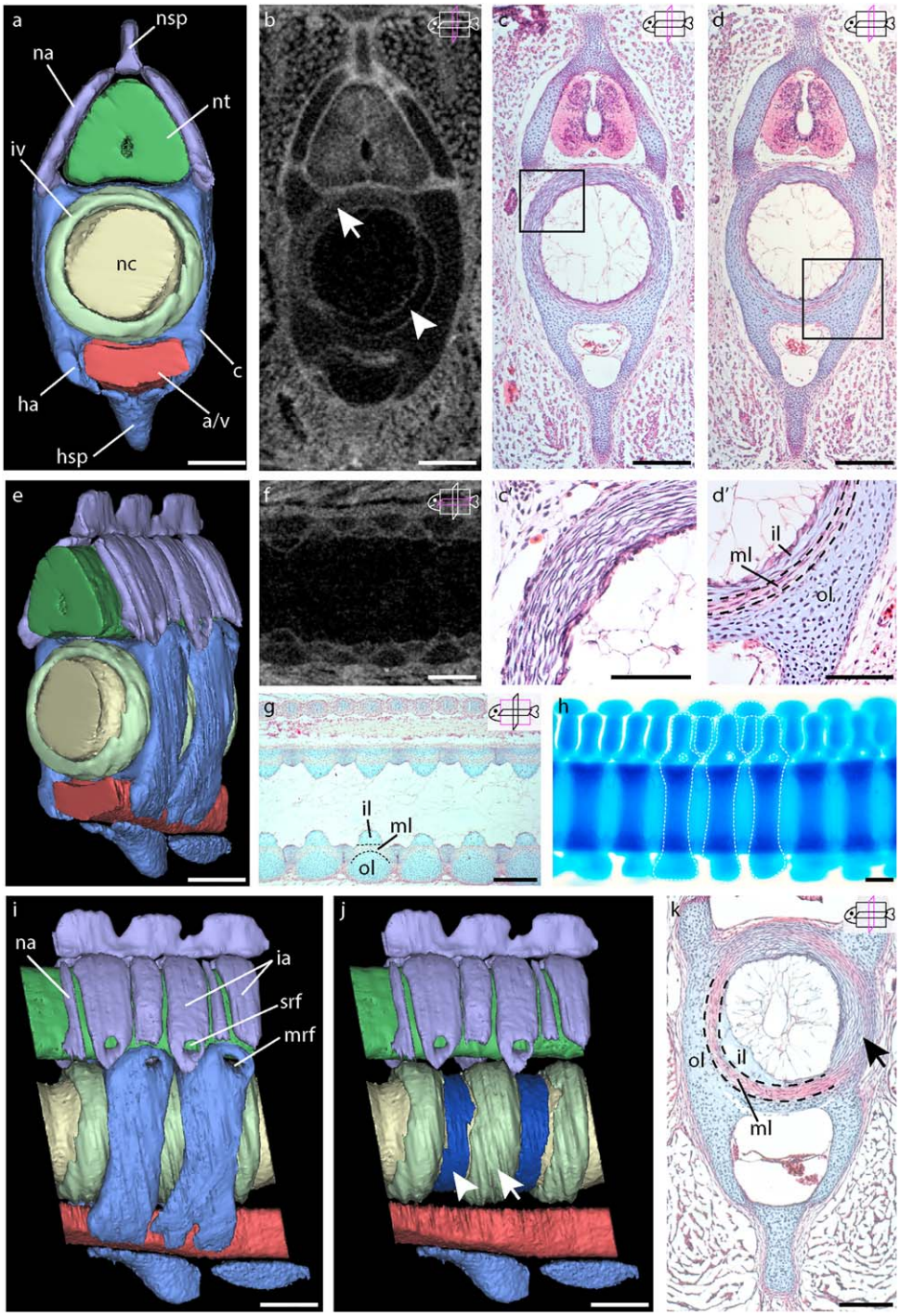

Fig. 8. *Leucoraja erinacea*, caudal embryonic vertebral morphology in Stage 32 embryos. **a**) anterior view of a CT reconstruction of the caudal vertebrae; **b**) transverse section through the IKI-stained CT scan, arrow indicates fibrous ring and arrowhead indicates mineralizing centrum; **c**) transverse section stained with HEA; **c′**) 20× magnification of the fibrous ring shown in c; **d**) transverse section stained with HEA and showing the mineralizing centrum; **d′**) 20× magnification of the incipient areolar calcification, indicated by the dashed lines; **e**) anterolateral view of the CT reconstruction; **f**) horizontal section through the CT scan; **g**) sagittal section stained with HEA and showing the early areolar calcifications and inner layer of cartilage; **h**) skeletal preparation of caudal vertebrae; **i**) lateral view of a CT scan of the caudal vertebrae; **j**) lateral view of a CT scan of the caudal vertebrae with outer cartilage removed to show the inner layer (arrowhead) and intervertebral region (arrow); **k**) transverse oblique section of a slightly older embryo showing both the mineralizing centrum and fibrous ring (arrow). a/v, caudal artery and vein, ca, cartilage, ha, hemal arch, hsp, hemal spine, ia, intercalary arch, il, inner layer of cartilage, iv, intervertebral region, ml, middle layer of the centrum/areolar calcification, mrf, motor nerve root foramen, na, neural arch, nsp, neural spine, nt, neural tube, ol, outer layer of hyaline cartilage, srf, sensory nerve root foramen. Icons in upper right corner indicate plane of section. Scale bars represent 200 μm for most images; scale bars represent 100 μm for c′ and d′.

sagittal and transverse CT sections the areolar tissue begins to substantially constrict the notochord (Fig. 7h,i). The middle layer of areolar tissue forms within the layer of spindle-shaped cells and is separate from the outer hyaline cartilage that envelops the notochord (Fig. 7c,c″,j,j′,k). Interestingly, this areolar calcification first forms just external to the notochord sheath in Stage 32 (Figs. 5c,c′ and 7c,c″), but in slightly older, Stage 33, embryos, a layer of chondrocytes sparsely embedded in Alcian blue-stained matrix (the "inner zone of vertebral development" of Ridewood, 1921) is present medial to the areolar calcification, suggesting that cartilage is differentiating on the inside of this mineralized tissue as well as on the outside (Fig. 7j,j′). These segmented centra, along with the inner layer of cartilage, have increased in size from Stage 31 and now substantially constrict the notochord in the center of each vertebral unit (Fig. 7h,i,j,j′). In the intervertebral regions, the fibrous rings have enlarged dramatically and surround the persistent notochord (Fig. 7a,c,c′,d,e,f,f′,g). The outer cartilage is no longer continuous, but is now present in the form of rectangle-shaped boxes that surround the centrum and notochord. The dorsolateral corners slant slightly posteriorly and contain spinal nerve foramina (Fig. 7d).

During Stage 32 several changes in vertebral morphology through the precaudal to caudal transition become more striking than in younger embryos. The same population of mesenchyme that condenses to form the transverse processes precaudally forms the hemal arches in the caudal region. Throughout the precaudal-caudal transition, in each successive vertebra, the transverse processes extend more and more ventrally until they are no longer transverse processes, but hemal arches (Fig. 8a; see Daniel (1922) for a clear figure of this transition in *Rhinobatis*). The caudal artery and vein are surrounded by the hemal arches laterally and dorsally, and are protected ventrally by hemal spines (Fig. 8a–e). The first hemal spine possesses two anterior prongs that cup the caudal artery and vein, as well as a median keel projecting ventrally (Fig. 8e). More posterior hemal spines are not as well developed and extend as a single rod of ventral cartilage throughout the tail. At this point, the hemal arches and spines are not continuous with each other as they were in previous stages. The fibrous rings, mineralized centrum, and matrix deposited medial to the centrum, are visible in both CT and histological section (Fig. 8b–d′,f,g).

Another visible difference between the caudal and precaudal regions includes a transition to the diplospondylic condition seen across elasmobranchs, in which two vertebrae are present in each myotomal segment. This change is visible in the spacing out of spinal nerve foramina, with one set of spinal nerves corresponding to each vertebral unit precaudally, but corresponding with two vertebral units in the caudal region (Fig. 8h–j). Neural and intercalary arches also change shape in relation to the re-spaced spinal nerves. Precaudal neural arches are slender and articulate to the dorsal margin of the vertebral cartilage, while the intercalary arches are much wider and support spinal nerve foramina ventrally. In the caudal region, however, both neural and intercalary arches adopt mostly the same shape, with the only differences in morphology being a slight expansion of the apex in the intercalary arches and the base in the neural arches (Figs. 7k and 8h). One neural spine is present for each set of neural and intercalary arches. The CT-reconstructions in Figure 8 (a,e,i,j) show that the anterior–posterior transition to caudal diplospondyly does not occur at the first appearance of hemal arches, but rather several vertebral segments posterior. The first several caudal vertebrae have hemal arches and spines, but both the relationship of spinal nerve foramina to vertebral cartilages and the neural arch morphology show the same pattern as the precaudal region. The whole mount, cleared and stained embryo (Fig. 8h) shows the more typical morphology of the arches in caudal vertebrae.

In transverse oblique HEA-stained sections of slightly older (Stage 33) embryos, all layers of the developing centrum are visible, including the inner layer, middle layer of areolar calcification, and outer layer of hyaline cartilage (Fig. 8k). The layer of fibrous, spindle-shaped cells that persist in the space between vertebral cartilages can also be seen in the intervertebral regions in oblique sections.

Stage 34+

By Stage 34 the vertebrae have taken on an adult-like morphology, with more sharply defined vertebral boundaries, mineralized centra, and a greatly reduced notochord (Figs. 9 and 10). The outer edges of the cartilage have begun to calcify as dense blocks of tesserae, which are easily visible in the slices of the microCT scans (Figs. 9b,e,h and 10b,d,e,g), and the mineralized centrum has dramatically increased in both length and width.

The arches in the precaudal region are well developed, and the large intercalary arches envelop most of the spinal cord (Fig. 9a–g). The sensory nerve roots exit the vertebral column through the foramina in the intercalary arches, while motor nerve roots exit through the dorsal portion of the outer hyaline cartilage (Fig. 9d,g). The neural arches are present as small slivers of cartilage that extend dorsally around the neural tube and expand at their bases to provide foramina for the exiting motor nerve roots. Neural spines are fully separated now, with expanded bases that articulate to the intercalary arches and wide dorsal margins, forming an elongate hourglass in cross

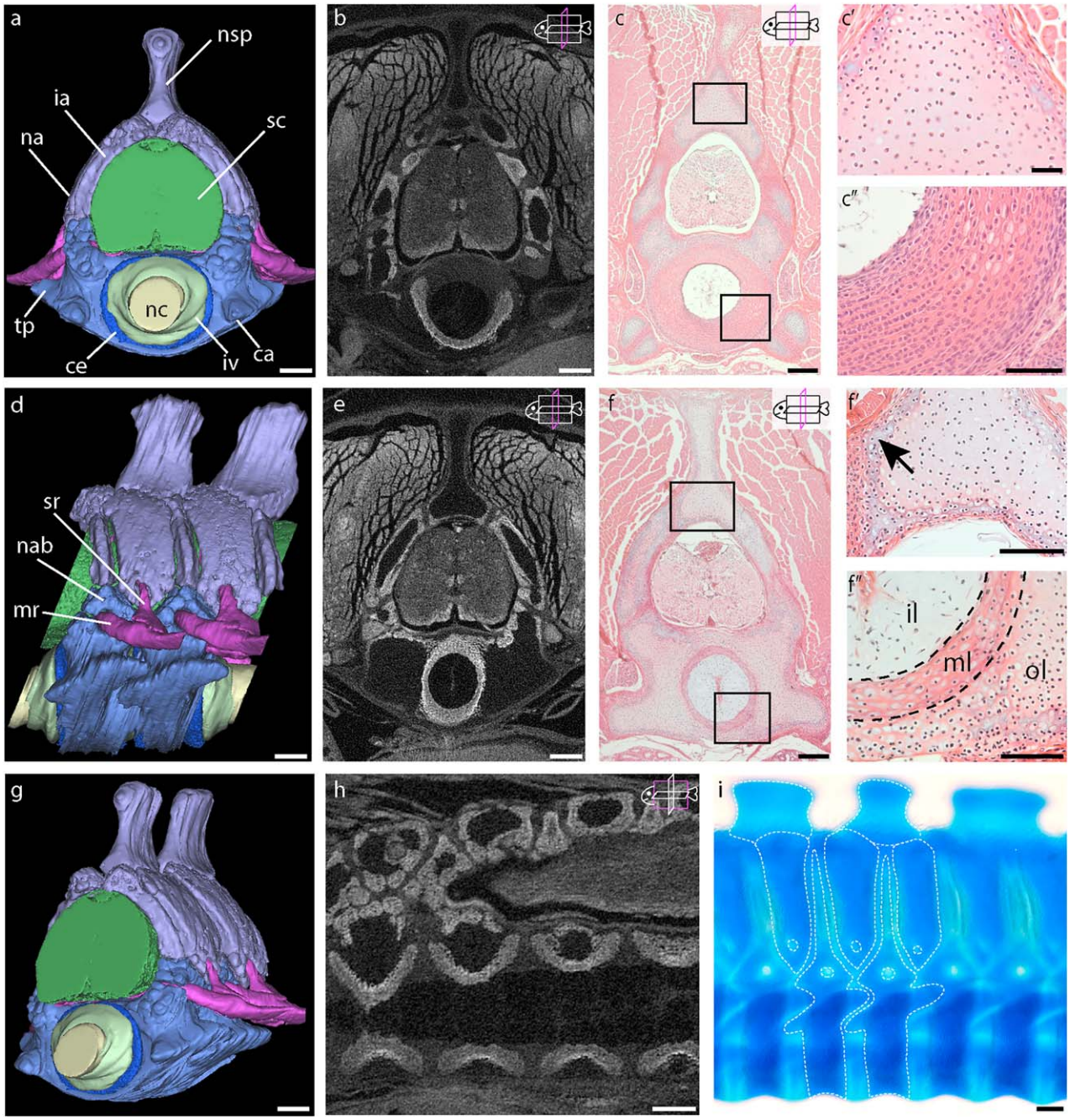

Fig. 9. *Leucoraja erinacea*, precaudal embryonic vertebral morphology in Stage 34. **a**) anterior view of a CT reconstruction of the vertebrae; **b**) transverse section through the IKI-stained CT scan showing the mineralizing centrum; **c**) transverse section stained with HEA; **c′**) 10× magnification of the neural spine cartilage; **c″**) 10× magnification of the areolar calcification of the centrum; **d**) lateral view of a CT reconstruction; **e**) transverse section through the CT scan showing the narrowest part of the centrum; **f**) transverse section stained with HEA and showing the narrowest part of the centrum; **f′**) 10× magnification of the neural spine cartilage, arrow indicates developing tesserae; **f″**) 10× magnification of the areolar calcification of the centrum; **g**) anterolateral view of the CT reconstruction; **h**) sagittal section of the CT scan; **i**) skeletal preparation of precaudal vertebrae showing transverse processes, neural arches, and intercalary arches. ca, outer cartilage, ce, centrum, ia, intercalary arch, il, inner layer of cartilage, iv, intervertebral region, ml, middle layer of cartilage/areolar calcification, mr, motor nerve root, na, neural arch, nab, neural arch base, nc, notochord, nsp, neural spine, nt, neural tube, ol, outer layer of hyaline cartilage, sr, sensory nerve root, tp, transverse process. Icons in upper right corner indicate plane of section. Scale bars represent 200 μm for most images; scale bars represent 100 μm for c′, c″, f′, and c″.

section (Fig. 9e). Histological sections show a fibrous perichondrium surrounding the hyaline cartilage of the arches and neural spines (Fig. 9c,c′,f,f′). Both sensory and motor nerve roots are large by this stage, to provide innervation to the anteroposteriorly expanded pectoral fins.

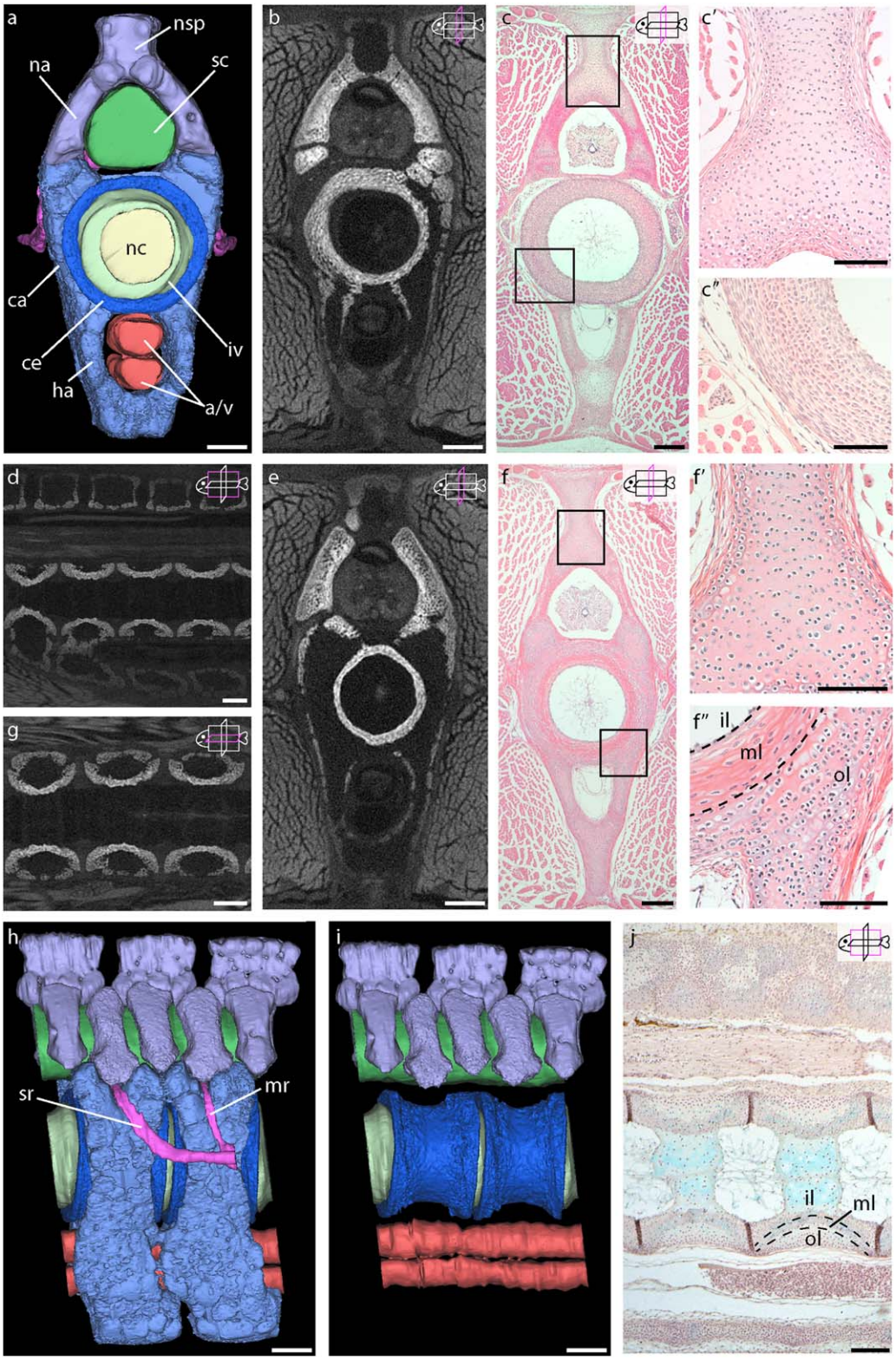

Fig. 10. *Leucoraja erinacea*, caudal embryonic vertebral morphology in Stage 34 embryos. **a**) anterior view of a CT reconstruction of the caudal vertebrae; **b**) transverse section through the IKI-stained CT scan showing the mineralizing centrum; **c**) transverse section stained with HEA; **c′**) 10× magnification of the neural spine cartilage; **c″**) 10× magnification of the areolar calcification of the centrum; **d**) sagittal section of the CT scan; **e**) transverse section of the CT scan showing the narrowest part of the centrum; **f**) transverse section stained with HEA and showing the narrowest part of the centrum; **f′**) 10× magnification of the neural spine cartilage; **f″** 10× magnification of f, dashed lines indicate middle layer/areolar calcification of the centrum; **g**) horizontal section through the CT scan; **h**) lateral view of a CT reconstruction; **i**) lateral view of the CT scan with outer cartilage removed; **j**) sagittal section stained with HEA, dashed lines indicate middle layer/areolar calcification. a/v, caudal artery and vein, ca, outer cartilage, ce, centrum, ha, hemal arch, il, inner layer of cartilage, iv, intervertebral region, ml, middle layer of the centrum/areolar calcification, mr, motor nerve root, na, neural arch, nc, notochord, nsp, neural spine, nt, neural tube, ol, outer layer of hyaline cartilage, sr, sensory nerve root. Icons in upper right corner indicate plane of section. Scale bars represent 200 μm for most images; scale bars represent 100 μm for c′, c″, f′, and c″.

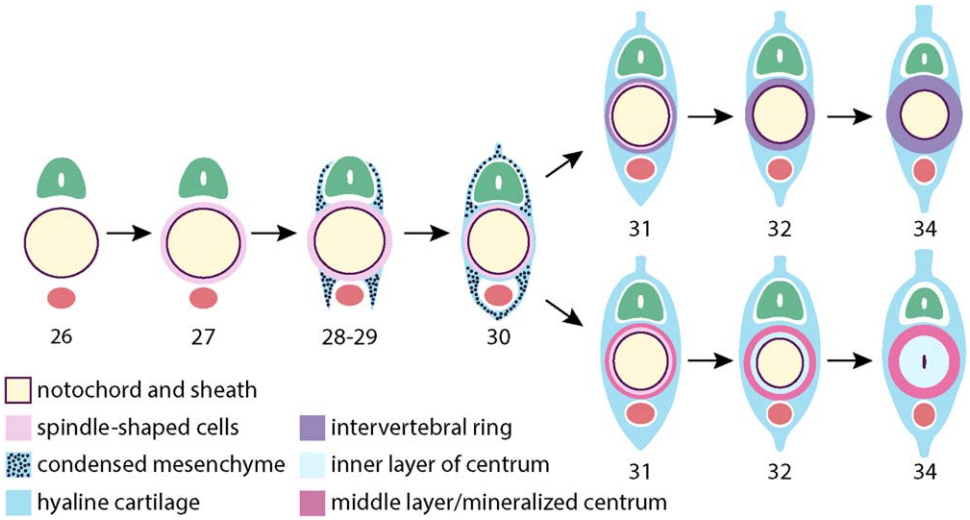

Fig. 11. Schematic showing the stages of vertebral development in the little skate, from Stages 27–34. The two rows on the right side of the schematic show cross sections of the intervertebral region (top) and the middle of a vertebra (bottom). Green = neural tube/spinal cord and red = caudal artery and vein.

Centra consist of a layer of outer, hyaline cartilage surrounding a middle layer of densely mineralized rings of areolar calcification (Fig. 9b,c,c″,e,f,f″,h,i). The inner layer of the centrum, situated between the notochord and the areolar calcification, has almost completely constricted the notochord in the center of each vertebra, leaving only a small notochordal canal in the center of these centra (Fig. 9f,f″). In section, these three layers stain differentially, with the outer cartilage staining light pink, the mineralized centrum staining a bright pink, and the third, inner layer remaining white or staining light blue (Fig. 9f″).

Similar to Stages 32 and 33 embryos, there are several differences in morphology between precaudal and caudal vertebrae in Stage 34 embryos. The neural spines are anteroposteriorly longer caudally than in the precaudal region, and have a more rectangular and block-like appearance with laterally expanding bases that articulate to both the neural and intercalary arches (Fig. 10a–e,h–j). The arches and outer cartilage of the centrum consist of hyaline cartilage with a peripheral layer of tesserae (Fig. 10c,c′,f–g).

The hemal arches have extended ventrally to fully enclose the caudal artery and vein (Fig. 9a), and individual vertebrae are completely separated from one another in the caudal region (Fig. 10h). Hemal arches and spines are fused together to form a single structure, but boundaries in the cartilages can still be seen in section (Fig. 10b,c,e,f). The hemal spines are offset slightly posteriorly from the hemal arches, and the most posterior portion of each hemal spine rests ventral to the anterior portion of the next set of hemal arches (Fig. 10h). The caudal mineralized centra are very similar to those in the precaudal region, showing a thin ring of areolar calcification in the center of each vertebral segment that thickens considerably near the anterior and posterior margins of each vertebra (Fig. 10c,c″,d,g,f,f″,i,j). The duplication of caudal vertebrae results in the presence of two vertebrae for each myotomal segment and in the increased spacing of spinal nerves (Fig. 10h). The neural and intercalary arches are similar in thickness in the caudal region, with the base of the neural arches articulating to the outer centrum cartilage to form spinal nerve foramina (Fig. 10h,i).

Summary of Vertebral Development in *Leucoraja erinacea*

The computed tomographic and histological analyses in this study provide a comprehensive view of vertebral development in the little skate. We show that a continuous layer of mesenchyme condenses around the notochord at Stage 27 and persists through vertebral development as a layer of spindle-shaped cells until it differentiates into the fibrous intervertebral rings and the areolar tissue in Stage 31 (Fig. 11). Beginning at Stage 28, mesenchymal cells condense around the neural tube and caudal artery and vein to form continuous neural arch and hemal arch tissues that extend the length of the axial column. During Stage 31, the neural and hemal arch mesenchyme differentiates into hyaline cartilage and surrounds the areolar tissue, where it will remain into adulthood. In Stage 32 arch cartilages subdivide into intercalary and neural arches and spines dorsally, and hemal arches and spines ventrally. An inner layer of cartilage forms medial to the areolar calcification, and substantially constricts the notochord. By Stage 34, the areolar calcification of the centrum is large and hourglass-shaped, and the

inner layer of cartilage almost completely constricts the notochord in the middle of each vertebral segment. In the intervertebral regions, the notochord persists into adulthood and is surrounded by the thickened ring of fibrous cells.

DISCUSSION

The Fibrous Sheath and Perichordal Tube

Several notable features were identified in the little skate in this study, including the initial formation of a continuous layer of spindle-shaped cells surrounding the notochord. This layer of cells subsequently differentiates into the areolar calcifications of the centra and the fibrous rings of the intervertebral regions. The spindle-shaped cells were first described as the thickened "fibrous sheath" of the notochord in several shark species, including *Squalus acanthias, Mustelus vulgaris*, and *Scyliorhinus canicula*, and this sheath was widely accepted as a derivative of the notochord epithelium (Gegenbaur, 1862; Gadow and Abbott, 1895). However, some researchers believed it to be sclerotome-derived, along with the rest of the vertebral components (Hasse, 1879; Klaatsch, 1893). In sharks, the fibrous sheath is bounded externally by the elastica externa, a thin membrane of intercrossing elastic fibers. The fibrous sheath is thought to be invaded in large numbers by sclerotomal cells that perforate the elastica externa at the bases of the neural and hemal arches and then divide and differentiate into cartilage within the sheath (Gadow and Abbott, 1895; Goodrich, 1930). Cross sections of Stage 27 skate embryos show mesenchymal cells condensing around the notochord prior to taking on an elongate spindle shape (Fig. 1), suggesting that the cells of the fibrous sheath are mesenchymal in origin. In sections of Stages 29 and 30 skate embryos, we were not able to easily identify the elastica externa or any cells that were in the process of migrating into the fibrous layer of spindle-shaped cells. Additionally, this layer of spindle-shaped cells is morphologically different than those described previously in sharks, with the cells having more irregular shapes and the layer including more extracellular matrix (Figs. 2c′,i′ and 3c′,j′; compare to Eames et al. (2007) Fig. 6). These differences imply that the fibrous sheath, previously identified to be a derivative of the notochord epithelium in sharks, in batoids develops from mesenchymal cells that have condensed around the notochord. If this is the case, then the areolar calcifications in skates do not form through sclerotomal cells invading a notochord-derived fibrous sheath (the process described in sharks by Gadow and Abbott, 1895), but rather through mesenchymal cells first differentiating into concentric layers of elongate cells and then calcifying.

Similar continuous condensations of tissue surrounding the notochord have been described in several other vertebrate taxa, such as salamander, chick, and mouse, in which they have been termed the perichordal tube (Williams, 1942; Williams, 1959; Wake and Lawson, 1973; Christ and Wilting, 1992). However, despite superficial similarities, there are important differences between the perichordal tube of tetrapods and the fibrous sheath of elasmobranchs. For example, in skate, the cells of the fibrous sheath become elongate and thin throughout the length of the axial column, running parallel to the notochord epithelium. The cells of the perichordal tube in chick, however, have the characteristic appearance of mesenchymal cells, and flatten into fibrous rings only at the intervertebral boundaries, early in vertebral development (Williams, 1942; Christ et al., 2000). This segmental thickening in chick occurs before the neural arches are fully developed. Similarly, in a plethodontid salamander, *Eurycea bislineata*, the perichordal tube is not consistent in diameter throughout the axial column, but rather forms thickened rings of elongate cells at incipient vertebral boundaries and thins to just one or two cells in the middle of each vertebral segment (Wake and Lawson, 1973). This unevenness contrasts with the fibrous sheath and the continuous cartilage of skates, which remains a constant thickness for several weeks of development, and does not subdivide until the neural and hemal arch mesenchyme has condensed and differentiated into cartilage.

It is unclear how widespread the perichordal tube is among vertebrates. Recent studies of the Japanese medaka (*Oryzias latipes*), a teleost fish, do not mention any layer of continuous tissue, but instead report that mesenchyme invades the notochord sheath at segmental intervals (e.g., Inohaya et al., 2007) and studies on vertebral development in other teleosts, such as zebrafish, do not discuss the condensation of sclerotomal mesenchyme in great detail (Morin-Kensicki et al., 2002; Fleming et al., 2004). However, there is some evidence of a thin tube of continuous mesenchyme in some teleost fishes. A thin layer of undifferentiated mesenchyme surrounding the notochord prior to centrum formation has been documented in Atlantic salmon, but, by the time centra begin to mineralize, neural and hemal arch cartilages are already well formed (Grotmol et al., 2003).

In addition to the notochord, mesenchyme also surrounds the neural tube in the form of unsegmented, nascent neural and intercalary arches in skate that differentiate into cartilage and later separate. We have found no evidence in the literature describing this continuous arch tissue in vertebrates outside sharks. Van Wijhe (1922) and De Beer (1924) documented the continuous early condensation of the neural arch mesenchyme in

Squalus acanthias and *Heterodontus francisci*, respectively, but these observations were later dismissed by Goodrich (1930) and "better ascribed to a temporary fusion of rudiments set very close together than to the arcualia having been evolved from an originally continuous cartilaginous band" (p. 16). Our observations, in the present work taken from histological sections and microCT scans of the little skate and in previous works observed in several species of sharks (van Wijhe, 1922; de Beer, 1924), are inconsistent with Gadow and Abbott's (1895) model of vertebral development in which pairs of basidorsal and interdorsal cartilages form the building blocks of the neural and intercalary arches. Using microCT scans and histology, we have shown here that in skate the earliest condensations of mesenchyme around the neural tube and caudal artery and vein are indeed continuous throughout the vertebral column length.

Subdivision of Initially Continuous Vertebral Cartilage

The mode of vertebral segmentation described in this study, in which segmented paraxial mesoderm migrates to condense around the notochord and neural tube, forms a continuous sleeve of cartilage that extends the entire length of the body, and then secondarily subdivides into discrete, repeating vertebral elements, has received minimal attention in the literature. Studies describing vertebral development in chick, mouse, and human mention a perichordal tube of condensed mesenchyme, but no mechanism to explain the secondary subdivision of this structure is proposed (Christ and Wilting, 1992; Wallin et al., 1994; Christ et al., 2000). It is possible that other segmented structures, such as spinal nerves and intersegmental blood vessels, drive perichordal tube subdivision, but little functional evidence exists to support this.

Segmentation of the perichordal tube in chick seems to take place when the incipient intervertebral discs begin to develop within the perichordal mesenchyme and replace the notochord (Christ and Wilting, 1992). These discs provide boundaries for developing vertebral centra, which later fuse to neural arch rudiments. In mammals, a similar process occurs, though the notochord is not completely replaced, but instead becomes the nucleus pulposus at the center of each intervertebral disc (Lefebvre and Bhattaram, 2010). In skate, cells within the fibrous sheath first differentiate into hyaline cartilage, which thickens substantially, before secondarily subdividing into vertebrae late in Stage 31.

The small bands of tissue that surround the notochord and correspond to nascent vertebral boundaries, as observed in one late Stage 31 skate embryo (Fig. 4b,j), might relate to the segmentation of the continuous vertebral cartilage in skate. The location of the bands at the widest part of the notochord, and just medial to the grooves in the dividing cartilage, is intriguing, and we speculate that these bands could represent iterative signaling centers that direct the subdivision of the tube of hyaline cartilage. Notochord segmentation has been proposed as a driver of centrum development in chick and in some teleost fishes (Stern, 1990; Grotmol et al., 2003). For example, in Atlantic salmon, calcification of the centrum seems to be initiated by the segmental organization of a layer of "chordoblast" cells located in the notochord sheath (Grotmol et al., 2005; Nordvik et al., 2005). In each vertebral segment these cells transition from an anteroposterior orientation to circular bands perpendicular to the AP axis. Subsequently, chordacentra begin to calcify in the notochord sheath at the position of these chordoblast bands, and sclerotomally derived osteoblasts begin to deposit bone on the surface of the chordacentra (Grotmol et al., 2003). However, beyond these morphological observations, the phenomenon of notochord segmentation is controversial: it has not been documented outside of a small number of teleost species (Grotmol et al., 2003, 2005; Haga et al., 2009), and an underlying molecular mechanism remains elusive.

The Composite Nature of the Axial Skeleton in Gnathostomes

Previous studies of skeletogenesis in sharks have identified three tissue layers early in the formation of the centrum, which is similar to what is documented in skate in this study (Daniel, 1922; Eames et al., 2007; Enault et al., 2015). These three layers, or zones of deposition, include an inner layer consisting of mostly extracellular matrix located superficial to the notochord, a middle layer of areolar calcification that forms the double cone of the centrum, and an outer layer of hyaline cartilage that is continuous with the arches and is jacketed with tesserae in adults. These layers stain differentially in later stage swell shark embryos (9 cm total length) (Eames et al., 2007) with the inner and outer layers staining with Safranin O and Alcian blue, indicating the presence of proteoglycans in the cartilage matrix, and the middle layer staining with Aniline blue, denoting the presence of collagen fibrils. Both the inner and middle layer, as well as the inner-most margin of the outer layer, showed alkaline phosphatase activity, which is indicative of mineralization. We recover the same three layers in the vertebrae of the little skate (Fig. 8f,f″), suggesting that centrum construction is similar across many elasmobranchs. As noted previously, however, in some sharks and batoids (the porbeagle shark *Lamna nasus*, the hammerhead *Sphyrna blochii*, the basking shark *Cetorhinus maximus*, and the guitarfish *Rhinobatos productus*) there is no outer layer of hyaline cartilage around the centrum;

hyaline cartilage is restricted to the arches (Ridewood, 1921; Daniel, 1922; Goodrich, 1930).

Multiple-part centra are known in many kinds of fishes. In most of these, the dual centrum complex consists of a chordacentral layer formed within the notochord sheath and an autocentrum consisting of a layer of bone deposited on the outside of the sheath and independent of the neural and hemal arches (Arratia et al., 2001). For example, the centrum of the fossil holostean *Ophiopsis* is formed from an autocentrous deposition of smooth and compact bone on the outside of the notochord sheath, as well as an inner chordacentrum containing one or two rings of small tubes (Bartram, 1975). The Jurassic teleost *Leptolepis* also has an inner chordacentrum with a smooth outer autocentrum (Arratia and Hikuroa, 2010). Similarly, centra in Atlantic salmon have been documented to form from an inner layer of cells located within the notochord sheath and an outer layer of bone that is deposited by mesenchymal cells (Nordvik et al., 2005). In the little skate, however, the outer centrum cartilage does not develop independently of the neural and hemal arches, but is continuous with them and forms via the same mesenchymal cell population. These various examples provide evidence that centrum development is often complex and difficult to document. Centra are not merely formed through a single process, but can develop through a combination of mineralization within the notochord sheath, as well as condensation of sclerotomal cells around the notochord and neural tube.

This variation in centrum construction raises questions about the embryonic origins of these different centrum components. As mentioned previously, fate mapping experiments in axolotl and chick have shown that tetrapod centra, along with the remainder of the vertebral skeleton, are derived from cells of the ventral somites (Bagnall et al., 1988; Piekarski and Olsson, 2014). However, the same does not seem to be entirely true for teleost fishes. The notochord appears to play a significant role in centrum development in Japanese medaka and Atlantic salmon, with a separate layer of centrum bone developing within the notochord sheath, independent of the sclerotome-derived skeletal tissue (Ekanayake and Hall, 1987; Nordvik et al., 2005). Even more compelling is the evidence from zebrafish, in which notochords have been shown to secrete bone matrix, and laser ablations of notochord cells result in the loss of centra (Fleming et al., 2004).

CONCLUSIONS

This study has comprehensively described the embryonic morphology and histology of the vertebral column in a skate for the first time. Histological and, in particular, 3D-microtomographic data have helped to elucidate the process of early mesenchymal condensation and differentiation. The anteroposteriorly continuous layer of cells that surrounds the notochord early in vertebral development appears to be mesenchymal in origin (likely derived from the sclerotome), and not derived from the notochord epithelium, as has been previously described in shark. It is possible that the notochord epithelium does play some role in inducing the formation of the layer of spindle-shaped cells, but additional experiments are necessary to test this. Additionally, rather than being separate structures at their genesis, neural arch mesenchyme initially condenses continuously throughout the anterior–posterior axis before separating into neural and intercalary arches. Centra have evolved independently in several clades of vertebrates (Arratia et al., 2001), and those separate origins are evident when comparing centrum development across taxa. Skate centrum construction is markedly differently from that of osteichthyans (e.g., zebrafish and chick), in that the centrum consists of three layers of tissue: the inner layer of cartilage that constricts the notochord, the areolar calcification that makes up the middle layer of the centrum, and an outer layer of hyaline cartilage. Zebrafish and chick centra both consist of one type of bone: acellular bone in the former and cellular bone in the latter (Hall, 2005).

We have provided critical information on the morphology and tissues present throughout skate vertebral development, but many broader questions remain unresolved, including the phylogenetic distributions of structures like the perichordal tube and composite centra, the embryonic origins of the centrum, and the mechanism driving the subdivision of the cartilaginous tube in elasmobranchs. These can be remedied with contrast-enhanced microCT, scans documenting axial column development across a broader range of taxa. Fate-mapping experiments to track the derivatives of both somites and the notochord in elasmobranchs will also be crucial in determining if the notochord makes a substantial and general (perhaps ancestral) contribution to centrum development in gnathostomes, or whether the notochord-derived centra of teleosts are unique. Additional morphological studies aimed at identifying segmental features of the notochord (such as the notochord bands or variations in notochord thickness) in other embryos, and experiments to identify and investigate the function of genes expressed segmentally along the notochord, will further test the role of the notochord in axial column segmentation.

When comparing vertebral development across gnathostomes, it becomes clear that this process is complex and variable within major taxa, and that Gadow and Abbott's (1895) "Arcualia Theory" of vertebral development does not apply to all

elasmobranchs, let alone all vertebrates. Features that were clearly defined in several different species of shark, including the elastica externa, seem to be absent in the little skate. These differences again underscore the fact that shark anatomy and development are not general for vertebrates. Rather, as the sister group to osteichthyans, developmental data from elasmobranchs can help to polarize character transformations within subgroups of the bony fishes. As vertebrae represent such a fundamental feature of the vertebrate body plan, their complex construction and independent evolutionary histories underpinning vertebral skeletal diversity provide an opportunity to study variation in the mechanisms of axial segmentation and the developmental basis of convergent evolution.

AUTHOR CONTRIBUTIONS

This project was conceived of and designed by KEC with advice from MIC and JAG. CT-scan analysis, histology, and skeletal preparations were completed by KEC. The manuscript was written by KEC with input from MIC and JAG.

ACKNOWLEDGMENTS

We thank Robert Ho, Melina Hale, and Haley Stinnett for valuable discussions and feedback on the manuscript. Scott Bennett and David Remsen at the Marine Biological Laboratory in Woods Hole, MA, provided *Leucoraja erinacea* embryos for this study. Jessie Maisano at the University of Texas High-Resolution X-Ray Computed Tomography Facility scanned some Stages 28–32 embryos. April Neander provided technical assistance with the GE CT scanner. We also thank Richard Behringer and Alejandro Sánchez Alvarado for support with lab space at the MBL. This project was supported by NSF DDIG DEB-1501749 and the MBL/UChicago Graduate Student Research Award.

LITERATURE CITED

Applegate SP. 1967. A survey of shark hard parts. In: Gilbert PW, Mathewson RF, Rall DP, editors. Sharks, Skates and Rays. Baltimore, Maryland: The Johns Hopkins Press. pp 37–67.

Arratia G, Hikuroa D. 2010. Jurassic fishes from the Latady Group, Antarctic Peninsula, and the oldest teleosts from Antarctica. J Vert Paleontol 30:1331–1342.

Arratia G, Schultze H-P, Casciotta J. 2001. Vertebral column and associated elements in dipnoans and comparison with other fishes: Development and homology. J Morphol 250:101–172.

Bagnall KM, Higgins SJ, Sanders EJ. 1988. The contribution made by a single somite to the vertebral column: Experimental evidence in support of resegmentation using the chick-quail chimaera model. Development 103:69–85.

Bartram AWH. 1975. The holostean fish genus *Ophiopsis* Agassiz. Zool J Linn Soc 56:183–205.

Bensimon-Brito A, Cardeira J, Cancela ML, Huysseune A, Witten PE. 2012. Distinct patterns of notochord mineralization in zebrafish coincide with the localization of Osteocalcin isoform 1 during early vertebral centra formation. BMC Dev Biol 12:28.

Christ B, Wilting J. 1992. From somites to vertebral column. Ann Anat 174:23–32.

Christ B, Huang R, Wilting J. 2000. The development of the avian vertebral column. Anat Embryol 202:179–194.

Daniel JF. 1922. The Elasmobranch Fishes. Berkeley, California: University of California Press. 334 p.

de Beer GR. 1924. Memoirs: Contributions to the study of the development of the head in *Heterodontus*. J Cell Sci s2–68: 39–65.

Dean MN, Summers AP. 2006. Mineralized cartilage in the skeleton of chondrichthyan fishes. Zoology 109:164–168.

Eames BF, Allen N, Young J, Kaplan A, Helms JA, Schneider RA. 2007. Skeletogenesis in the swell shark *Cephaloscyllium ventriosum*. J Anat 210:542–554.

Ekanayake S, Hall BK. 1987. The development of acellularity of the vertebral bone of the Japanese medaka, *Oryzias latipes* (Teleostei; Cyprinidontidae). J Morphol 193:253–261.

Enault S, Muñoz DN, Silva WTAF, Borday-Birraux V, Bonade M, Oulion S, Ventéo S, Marcellini S, Debiais-Thibaud M. 2015. Molecular footprinting of skeletal tissues in the catshark *Scyliorhinus canicula* and the clawed frog *Xenopus tropicalis* identifies conserved and derived features of vertebrate calcification. Front Genet 6. doi: 10.3389/fgene.2015.00283.

Fischer AH, Jacobson KA, Rose J, Zeller R. 2008. Hematoxylin and eosin staining of tissue and cell sections. CSH Protoc 2008:pdb.prot4986.

Fleming A, Keynes R, Tannahill D. 2004. A central role for the notochord in vertebral patterning. Development 131:873–880.

Fleming A, Kishida MG, Kimmel CB, Keynes RJ. 2015. Building the backbone: The development and evolution of vertebral patterning. Development 142:1733–1744.

Gadow H. 1933. The Evolution of the Vertebral Column. Cambridge: Cambridge University Press. 356 p.

Gadow H, Abbott EC. 1895. On the evolution of the vertebral column of fishes. Philos Trans R Soc Lond B 186:163–221.

Gegenbaur C. 1862. Untersuchungen zur vergleichenden Anatomie der Wirbelsaule bei Amphibien and Reptilien. Leipzig: Wilhelmn Engelmann. 71 p.

Gillis JA, Dahn RD, Shubin NH. 2009. Chondrogenesis and homology of the visceral skeleton in the little skate, *Leucoraja erinacea* (Chondrichthyes: Batoidea). J Morphol 270:628–643.

Goodrich E. 1930. Studies on the Structure and Development of Vertebrates. London: Dover Publications. 837 p.

Grotmol S, Kryvi H, Nordvik K, Totland GK. 2003. Notochord segmentation may lay down the pathway for the development of the vertebral bodies in the Atlantic salmon. Anat Embryol 207:263–272.

Grotmol S, Nordvik K, Kryvi H, Totland GK. 2005. A segmental pattern of alkaline phosphatase activity within the notochord coincides with the initial formation of the vertebral bodies. J Anat 206:427–436.

Haga Y, Dominique VJ, Du SJ. 2009. Analyzing notochord segmentation and intervertebral disc formation using the twhh: gfp transgenic zebrafish model. Transgenic Res 18:669–683.

Hall BK. 2005. Bones and Cartilage: Developmental and Evolutionary Skeletal Biology. San Diego, California: Elsevier Academic Press. 760 p.

Hasse K. 1879. Das natürliche System der Elasmobranchier auf Grundlage des Baues und der Entwicklung ihrer Wirbelsäule: eine morphologische und paläontologische Studie. Jena: Gustav Fischer. 284 p.

Inohaya K, Takano Y, Kudo A. 2007. The teleost intervertebral region acts as a growth center of the centrum: In vivo visualization of osteoblasts and their progenitors in transgenic fish. Dev Dyn 236:3031–3046.

Jarvik E. 1980a. Basic Structure and Evolution of Vertebrates. London: Academic Press. 575 p.

Jarvik E. 1980b. Basic Structure and Evolution of Vertebrates. London: Academic Press. 337 p.

Klaatsch H. 1893. Beitrage zur vergleichenden Anatomie der Wirbelsaule. I. Ueber den Urzustand der Fischwirbelsaule. Morphologisches Jahrbuch 19:649–680.

Klymkowsky MW, Hanken J. 1991. Whole-mount staining of *Xenopus* and other vertebrates. Methods Cell Biol 36:419–441.

Lefebvre V, Bhattaram P. 2010. Chapter Eight—Vertebrate Skeletogenesis. In: Koopman P, editor. Current Topics in Developmental Biology, Vol. 90. San Diego, CA: Academic Press. pp 291–317.

Maxwell EE, Fröbisch NB, Heppleston AC. 2008. Variability and conservation in late chondrichthyan development: Ontogeny of the winter skate (*Leucoraja ocellata*). Anat Rec 291:1079–1087.

Miles RS. 1970. Remarks on the vertebral column and caudal fin of acanthodian fishes. Lethaia 3:343–362.

Morin-Kensicki EM, Melancon E, Eisen JS. 2002. Segmental relationship between somites and vertebral column in zebrafish. Development 129:3851–3860.

Nordvik K, Kryvi H, Totland GK, Grotmol S. 2005. The salmon vertebral body develops through mineralization of two preformed tissues that are encompassed by two layers of bone. J Anat 206:103–114.

Owen R. 1848. On the Archetype and Homologies of the Vertebrate Skeleton. London: Richard and John E. Taylor. 203 p.

Piekarski N, Olsson L. 2014. Resegmentation in the mexican axolotl, *Ambystoma mexicanum*. J Morphol 275:141–152.

Ridewood W. 1921. On the calcification of the vertebral centra in sharks and rays. Philos Trans R Soc Lond B 210:311–407.

Ridewood WG. 1899. Some observations on the caudal diplospondyly of sharks. Zool J Linn Soc Lond 27:46–59.

Schaeffer B. 1967. Osteichthyan vertebrae. Zool J Linn Soc Lond 47:185–195.

Stern CD. 1990. Two distinct mechanisms for segmentation? Semin Dev Biol 1:109–116.

van Wijhe JW. 1922. Frühe Entwicklungsstadien des Kopf- und Rumpfskeletts von *Acanthias vulgaris*. Bijdragen tot de Dierkunde 1922:271–298.

Wake DB, Lawson R. 1973. Developmental and adult morphology of the vertebral column in the plethodontid salamander *Eurycea bislineata*, with comments on vertebral evolution in the Amphibia. J Morphol 139:251–299.

Wallin J, Wilting J, Koseki H, Fritsch R, Christ B, Balling R. 1994. The role of *Pax-1* in axial skeleton development. Development 120:1109–1121.

Wang S, Kryvi H, Grotmol S, Wargelius A, Krossøy C, Epple M, Neues F, Furmanek T, Totland GK. 2013. Mineralization of the vertebral bodies in Atlantic salmon (*Salmo salar* L.) is initiated segmentally in the form of hydroxyapatite crystal accretions in the notochord sheath. J Anat 223:159–170.

Williams EE. 1959. Gadow's arcualia and the development of tetrapod vertebrae. Q Rev Biol 34:1–32.

Williams JL. 1942. The development of cervical vertebrae in the chick under normal and experimental conditions. Am J Anat 71:153–179.